



Review article

A review on development and modification strategies of MOFs Z-scheme heterojunction for photocatalytic wastewater treatment, water splitting, and DFT calculations

Narges Elmi Fard^a, Nisreen S. Ali^b, Noori M. Cata Saady^c, Talib M. Albayati^{d,*}, Issam K. Salih^e, Sohrab Zendejboudi^f, Hamed N. Harharah^g, Ramzi H. Harharah^h

^a Department of Chemistry, Science and Research Branch, Islamic Azad University, Tehran, Iran

^b Materials Engineering Department, College of Engineering, Mustansiriyah University, Baghdad, Iraq

^c Department of Civil Engineering, Memorial University, St. John's, NL, A1B 3X5, Canada

^d Department of Chemical Engineering, University of Technology- Iraq, 52 Alsinaa St., PO Box, 35010, Baghdad, Iraq

^e Department of Chemical Engineering and Petroleum Industries, Al-Mustaqbal University College, Babylon, 51001, Iraq

^f Department of Process Engineering, Memorial University, St. John's, NL, A1B 3X5, Canada

^g Department of Chemical Engineering, College of Engineering, King Khalid University, Abha 61411, Kingdom of Saudi Arabia

^h Department of Chemical and Process Engineering, Faculty of Engineering & Built Environment, Universiti Kebangsaan Malaysia, 43600 Bangi, Selangor, Malaysia

ARTICLE INFO

Keywords:

MOFs Z-scheme heterojunction
Photocatalytic
Degradation
Wastewater treatment
Water splitting

ABSTRACT

Increasing water pollution and decreasing energy reserves have emerged as growing concerns for the environment. These pollution are due to the dangerous effects of numerous pollutants on humans and aquatic organisms, such as hydrocarbons, biphenyls, pesticides, dyes, pharmaceuticals, and metal ions. On the other hand, the need for a clean environment, finding alternatives to fossil and renewable fuels is very important. Hydrogen (H₂) is regarded as a viable and promising substitute for fossil fuels, and a range of methodologies have been devised to generate this particular source of energy. Metal-organic frameworks (MOFs) are a new generation of nanoporous coordination polymers whose crystal structure is composed of the juxtaposition of organic and inorganic constituent units. Due to their flexible nature, regular structure, and high surface area, these materials have attracted much attention for removing various pollutants from water and wastewater, and water splitting. MOFs Z-scheme heterojunctions have been identified as an economical and eco-friendly method for eliminating pollutants from wastewater systems, and producing H₂. Their low-cost synthesis and unique properties increase their application in various energy and environment fields. The heterojunctions possess diverse properties, such as exceptional surface area, making them ideal for degradation and separation. The development and formulation of Z-scheme heterojunctions photocatalytic systems using MOFs, which possess stable and potent redox capability, have emerged as a successful approach for addressing environmental pollution and energy shortages in recent times. Through the utilization of the benefits offered by MOFs Z-scheme heterojunctions photocatalysts, such as efficient separation and migration of charge carriers, extensive spectrum of light absorption, among other advantages, notable enhancements can be attained. This review encompasses the synthesis techniques, structure, and properties of MOFs Z-scheme heterojunctions, and their extensive use in treating various

* Corresponding author.

E-mail address: talib.m.naieff@uotechnology.edu.iq (T.M. Albayati).

wastewaters, including dyes, pharmaceuticals, and heavy metals, and water splitting. Also, it provides an overview of the mechanisms, pathways, and various theoretical and practical aspects for MOFs Z-scheme heterojunctions. Finally, it thoroughly assesses existing challenges and suggests further research on the promising applications of MOFs Z-scheme in industrial-scale wastewater treatment.

1. Introduction

Pollutants in water bodies have raised concerns regarding their impact on the ecosystem and human health, despite water covering a large portion of the Earth's surface, only a small fraction is useable, with much being contaminated [1,2]. The degradation of underground water quality in densely populated areas can be attributed to increased use of chemical compounds and the inadvertent seepage of residential and industrial waste, highlighting a significant decline in such water resources. To address this issue, reverse osmosis membranes are widely utilized for efficient removal of elements, particularly toxic metal ions, while porous adsorbents are employed to achieve high adsorption performance [3–6]. Metal oxides [7–13], metal sulfides [14,15], carbons, zeolites, and porous organic frameworks, particularly metal-organic frameworks (MOF), are some of the adsorbents employed for this objective. MOFs have garnered significant attention as a novel material due to their structural characteristics and adsorption capacity. The high carbon content in MOF organic ligands enables their use as a template and a carbon precursor, eliminating the need for additives [16]. MOFs are extensive networks consisting of metal centers connected by organic bonds, and their physical and chemical characteristics are influenced by the arrangement of ligands and metals in two-dimensional (2D) and three-dimensional (3D) forms, allowing them to serve as unique adsorbents capable of trapping, retaining, and releasing molecules through small pores or open channels, and the synthesis of these materials grants control over the size, shape, and perimeter of the pores, resulting in enhanced selectivity [17]. MOFs have potential in different fields, including surface adsorption, energy storage, photocatalysis, water splitting, sensors, and biotechnology. The presence of many holes in MOFs causes these materials to host catalytically active species called guest molecules; therefore, they are considered a suitable option for photocatalytic applications [18]. The architectural and configurational attributes of MOFs are heavily influenced by critical factors such as the molar ratio of the reactants, the characteristics of the solvents employed, the pH conditions, as well as the temperature. As a result, these factors endow MOFs with distinct properties [19]. UiO-66, MIL-125, and MOF-5 are among the promising MOFs for photocatalysis. MOF composites are composed of a unique combination of organic ligands and metal-oxo clusters, which play distinct roles as light-absorbing antennas and isolated semiconductor quantum dots (QDs), respectively [20]. The inherent modular nature of MOFs greatly facilitates the fine-tuning and customization of various components within their structures, including metal templates, organic linkers, channels, and framework pores. This exceptional level of control over the fundamental building blocks of MOFs enables researchers and scientists to precisely engineer and optimize their properties and functions, improving photocatalytic performance and potential applications in different fields, such as solar energy conversion, water splitting, and pollutant degradation [21]. The employment of MOFs as photocatalytic agents has attracted considerable attention due to their versatile structural design and unique physical and chemical properties, differentiating them from conventional photocatalysis [22]. Significantly, a range of MOFs, such as MIL-53(Fe), MIL-68(Fe), and MIL-100(Fe), exhibit noteworthy absorption properties within the visible (VIS) light spectrum. This phenomenon can primarily be ascribed to the inclusion of metal-exo clusters in their structural composition [23]. Recent studies have demonstrated the efficacy of incorporating metal oxides and metal sulfides with MOF to enhance their photocatalytic activity [24]. The synergistic combination, which refers to the simultaneous effect of two or more components working together, has been experimentally demonstrated to enhance the overall performance of the photocatalytic system remarkably. This substantial increase in efficiency has been observed through numerous research studies, indicating a positive correlation between the combined components and the desired outcome [24]. The enhanced effectiveness can be ascribed to the dissemination of semiconductors within the porous and permeable structure of the MOF, thus generating heterojunctions and enhancing their functionality [24]. These heterojunction connections play an important role in increasing the performance of photocatalysts by initiating and facilitating photocatalytic reactions. Moreover, the conduction band (CB) position, capacitance, and n-p type characteristics significantly affect the formation of these heterojunctions. In addition, these connections help to isolate the load and contribute to the long life of the load carriers [25–27]. Consequently, the heterojunction method effectively connects semiconductors with narrow optical gaps and is a simple yet highly effective approach to enhance electron transfer and prevent electron-hole recombination. As a result, it increases the overall photocatalytic efficiency [28]. Notably, many semiconductor metal oxides and sulfides, including TiO₂, ZnO, BiVO₄, Ag₃PO₄, CdS, MoS₂, and Fe₂O₃, have found wide applications as photocatalysts for wastewater treatment [29–35]. Several studies have confirmed that incorporating MOFs into the crystal structure of these semiconductors leads to synergistic effects and thus improves the photocatalytic properties [36].

The process of solar light-assisted water splitting, which utilizes MOF-based heterojunction photocatalysts, has gained significant recognition as a highly promising technique in tackling the pressing challenges pertaining to energy and the environment. The concept of water splitting, owing to its environmentally friendly characteristics, has garnered considerable interest as an appealing approach for harnessing and storing substantial quantities of solar energy in the form of chemical compounds [37,38]. The process of water splitting can be accomplished by utilizing heterojunction photocatalysts based on MOFs, provided that a photon with an energy level exceeding the band gap (BG) energy of the MOF-based heterojunction photocatalysts is provided. Furthermore, it has been proposed that the lowest region of the semiconductor's CB edge should exhibit a more negative value compared to the reduction potential [38]. A specific category of MOFs Z-scheme heterojunction has the capacity to produce electrons and holes in two semiconductors at lower

energy levels, thus decreasing recombination and enhancing their effectiveness as photocatalysts for visible light absorption. These innovative MOFs Z-scheme heterojunction outshine traditional approaches in treating wastewater pollutants in sunlight by effectively breaking down large molecular pollutants like dyes found in industrial wastewater. MOFs Z-scheme heterojunction photocatalysts offer a cost-efficient solution for mitigating water pollution under visible light by excelling in the efficient splitting of water molecules, a common challenge for most photocatalysts responsive to visible light [37,38].

The purpose of the review is to fully cover the complex synthesis process of MOF materials, elucidate the diverse range of their properties, and investigate their potential applications in various fields. In particular, it addresses the fascinating realm of applications and properties of MOFs in wastewater treatment and further highlights their importance and potential contribution to this advanced field of study. Furthermore, it emphasizes the importance of modified MOFs with a special focus on their heterojunction design and their vital role in removing various pollutants, and water splitting; thus, their pivotal role in addressing environmental concerns is emphasized. In addition, this comprehensive review discusses use of compact density functional theory (DFT) calculations to probe the heterojunction nature of MOFs, which allows extensive investigation of important aspects such as electron and band structure (BS), valence band (VB) maximum, CB minimum, and precise orientation. It provides electron migration and complex elimination pathways. Finally, it presents the challenges, prospects, and promising research avenues to enhance understanding of the MOFs Z-scheme heterojunctions and advance their practical applications.

2. Metal-organic frameworks (MOFs)

Porous materials, including activated carbon, zeolite, polymer foams, ceramics, metal, and porous glass, have found extensive use in various aspects of our everyday existence. The realm of porous materials, especially those with nanoporosity, has seen significant growth and development over the past two decades. This growth can be primarily attributed to these materials' commendable stability properties [39]. With their exceptional ability to facilitate the flow of liquids and gases through interconnected pores and channels, these materials have proven useful in various fields such as adsorption and separation, photocatalysts, water splitting, energy storage, and environmental improvement [39]. MOFs, commonly known for their distinctive ability to form complex 3D crystalline structures, have emerged as prominent contenders among various porous materials developed in recent years, primarily due to their remarkable porosity and thermal stability. With the strategic selection of different building blocks, MOFs are designed with the possibility of achieving specific pore size, surface area, and functions [40,41]. The distinctive properties exhibited by MOFs have attracted considerable attention, and more than 20,000 distinct MOF structures are being studied and investigated. Fig. 1 provides a visual representation and examples of the various MOF structures discovered.

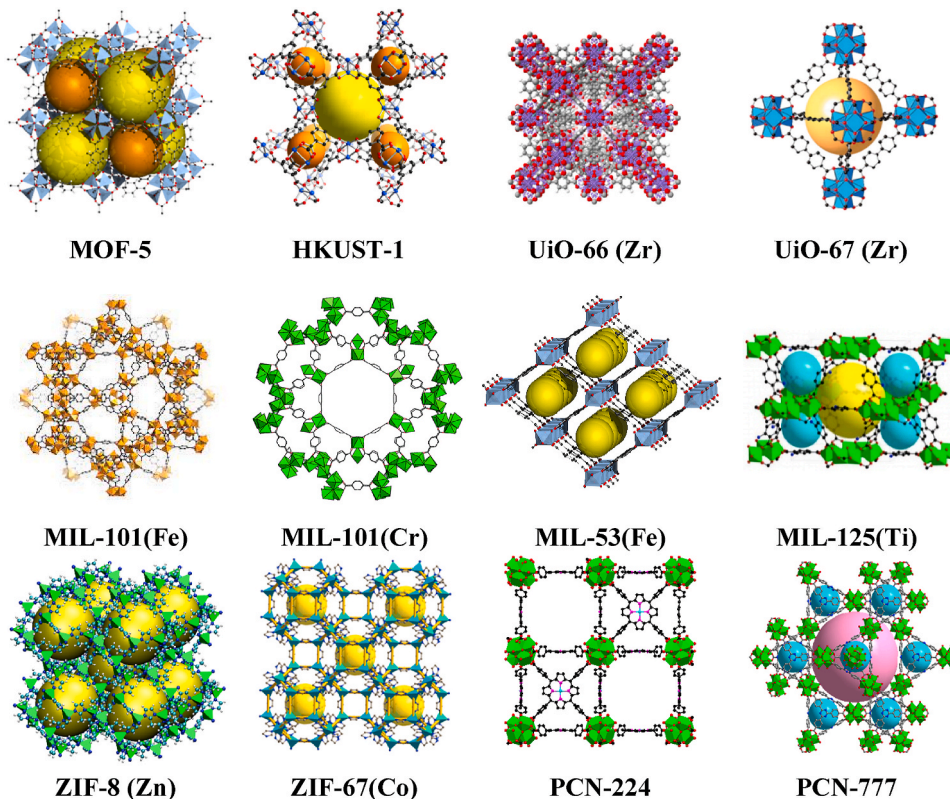


Fig. 1. Different MOFs with nano-porous structures [40,41].

A group of researchers led by Yaghi successfully produced a framework material known as MOF-5 by combining metal and organic ligands [42]. This marked the inception of MOFs, a novel type of material that has garnered significant attention from researchers. MOFs are characterized by their porous nature, which arises from intramolecular pores created by coordinating the formation of metal ion nodes or clusters with several organic ligands serving as supports [43].

The researchers' in-depth investigations have provided valuable insights into MOFs' deep versatility and wide relevance in many fields, including chemistry, chemical industry, biology, and materials science. MOFs have undoubtedly exhibited remarkable effectiveness and unparalleled efficacy in diverse domains, encompassing but not restricted to energy storage, photocatalytic activity, water splitting, surface adsorption, and drug delivery. It is worth noting that the groundbreaking discovery of the exceptional ability of MOF-5 to degrade phenol when exposed to ultraviolet (UV) light led to extensive research efforts aimed at investigating the potential of MOFs in the field of photocatalytic degradation of wastewater pollutants, especially organic substances that significantly challenged traditional purification processes. In this context, detailed research on MOFs such as zeolite imidazolate frameworks (ZIFs), University of Oslo (UiOs), and Lavoisier Institute (MIL) materials to evaluate their effectiveness in reducing the presence of organic pollutants such as hydrocarbons, biphenyls, pesticides, phenols, drugs, and dyes has been conducted [44]. The promising properties of MOFs make them attractive as photocatalysts, and one of the vital features is their excellent specific surface area, which greatly facilitates photocatalytic processes. In addition, MOFs exhibit unique porosity that allows the compatibility of various guest molecules and increases their versatility in catalytic reactions when used as photocatalysts [45]. The researchers have observed that combining organic compounds and metal clusters in MOFs creates a synergistic effect, thus improving light absorption capacity and increasing photocatalytic degradation efficiency. This is achieved through ligand-to-metal and metal-to-ligand charge transfer processes, commonly called LMCT and MLCT, respectively [46]. These charge transfer mechanisms contribute to the overall MOFs efficiency as photocatalysts. As a result of these key properties, MOFs have become very important as superior photocatalysts in energy and environmental applications [47]. Compared to a wide range of conventional photocatalysts such as metal nitrides [48], metal oxides [49–52], QDs [53], carbon materials [54], metal sulfides [55,56], phosphides [57], layered double hydroxides (LDHs) [58], and graphitic carbon nitride (g-C₃N₄) [59], MOFs as a particular type of photocatalyst are considered more practical and have demonstrated greater success. Conventional photocatalysts have faced several obstacles in their application, including insufficient utilization of sunlight, limited access to active sites, and insufficient understanding of the complex interaction between photocatalyst structure and photocatalytic activity [60]. However, MOFs have demonstrated high photon trapping efficiency, large surface area, and adjustable porosity that could potentially mitigate these issues. This has led to exploring MOF derivatives to investigate their diverse physical and chemical properties and expand their multifaceted applications. The less restrictive nature of scientific/research investigations has facilitated this pursuit [61]. Table 1 compares the performance of several photocatalysts with that of MOF photocatalysts in removing Methylene Blue (MB) azo dye. The high efficiency and shorter duration of MOF-based photocatalysts in the removal of MB compared to other photocatalysts clearly show the significant effectiveness of MOFs in the purification process.

2.1. MOFs synthesis methods, characteristics, and applications

Synthesis methods. Various techniques for synthesizing microporous MOFs are available in the scientific literature, each possessing unique merits and demerits. Among these methods, the solvothermal/hydrothermal technique is popular for fabricating microporous MOFs, wherein reactions are carried out under elevated temperatures and pressures [71]. In fact, using this method brings numerous advantages, in particular, achieving high levels of crystallinity in the fabricated structures and the ability to fine-tune the size and morphology of the particles [72]. However, this method requires long periods for the reactions, along with the essential requirements of using organic solvents and applying enormous pressures and temperatures. An alternative technique, commonly known as microwave-assisted synthesis, is widely recognized as a simple and rapid approach that is routinely used to produce small and uniform particles [73]. Despite its numerous advantages, the emergence of a secondary phase during the process is a prominent drawback of this method. Sonochemical synthesis has produced small nanocrystals with superior crystallinity as an alternative synthesis route [74]. Moreover, the field of electrochemical synthesis, known for its distinctive capability to produce a MOF thin film, remains enigmatic regarding the fundamental mechanisms responsible for its observed phenomena and behaviors. In this regard, the mechanistic approach represents a suitable alternative method for MOF synthesis, which provides a means to fabricate MOF and hybrid crystals without undesirable impurities and with minimal solvent use [75]. This innovative and new approach offers a promising and desirable method for synthesizing different types of MOFs. It offers many potential advantages in terms of purity and efficiency, as reported in

Table 1
Efficiency of various photocatalysts in removing MB azo dye.

Materials	Time (min)	Degradation Efficiency (%)	Ref.
Fe(II) on the g-C ₃ N ₄ /CDs	60	57–66	[62]
FeO	35	90	[63]
Fe ₂ O ₃	30	97	[64]
γ-Fe ₂ O ₃ @ GO	60	90	[65]
Born-GO-CuS	60	95	[66]
Cu ₉ S ₅	240	79	[67]
UiO-66/MIL-101(Fe)	120	99	[68]
CoFe ₂ O ₄ /SiO ₂ /Cu-MOF	60	98	[69]
NiCuZr/MIL-101(Fe)-NH ₂	10	98	[70]

the literature [76]. However, it should be noted that this particular method may require using solvents in the purification step, which should not be overlooked. In addition, increasing the production of MOFs using this technique poses several challenges that should be carefully investigated. It is worth noting that the mechanochemistry performed so far has been limited to the laboratory scale and has not yet been successfully implemented on an industrial scale. Therefore, it needs further exploration and development. As a final method for MOF synthesis, microemulsion synthesis appears to be an attractive and useful option that allows the creation of various MOFs with precise compositions and morphologies. However, it should be acknowledged that the presence of solvents, surfactants, and the relatively low reaction yields pose significant challenges to the overall effectiveness of this approach [77]. Finally, the selection and implementation of various methods for MOF synthesis should be made based on a comprehensive evaluation of several factors such as temperature, time, type of solvent, and the desired type of MOF produced, taking into account the advantages and disadvantages associated with each specific method [78,79]. Flow chemistry has emerged as a prominent synthesis technique for various MOFs in recent years. Differing from traditional batch reactions, flow chemistry entails a continuous stream of chemical reactions within a tube, offering benefits such as enhanced heat and mass transfer, precise management of reaction variables, and the ability to operate under harsh conditions safely. This approach is cost-effective, environmentally sustainable, and well-suited for industrial-scale production owing to its efficient transport characteristics, reduced solvent and energy consumption, as well as seamless integration of downstream processes and quality assurance protocols [80].

Table 2 comprehensively describes the synthesis methods used, relevant conditions, and reaction times for various MOFs.

Fig. 2 illustrates the advantages and disadvantages of different techniques used in the synthesis of MOFs.

Characteristics. There are several strategies to provide a comprehensive understanding of the interaction of MOFs and other materials through structural characterization. Various characterization techniques have been developed and implemented [94]. Different techniques, such as X-ray diffraction (XRD), are employed to identify and determine the structure of crystalline materials. Other techniques, including Fourier transform infrared spectroscopy (FTIR), are used to identify functional groups and determine the structure of organic species and Raman spectroscopy to identify molecules, while scanning electron microscopy (SEM) is used to evaluate surface morphology. In addition, diffuse reflectance spectroscopy (DRS) to study the optical properties of materials and the Bronner-Emmett Teller (BET)/Bart-Joyner-Hallanda (BJH) theory as a means to measure the specific surface area, pore size, and pore distribution are used. Also, photoluminescence (PL) is employed to assess materials' electronic and optical properties. X-ray photoelectron spectroscopy (XPS) is another useful technique to measure and determine materials' chemical composition and bond type. Finally, electron paramagnetic resonance (EPR) is used to identify unpaired electrons in the material under investigation [94]. Various techniques for material characterization are frequently employed in electrochemistry, such as cyclic voltammetry (CV), linear sweep voltammetry (LSV), impedance, and Mott-Schottky analysis. These methods are extensively utilized in the fields of electrochemistry and analytical chemistry. Fig. 3 provides a comprehensive depiction of the various methodologies employed in the synthesis of MOFs, the characterization techniques commonly utilized, the mechanical pathway implicated, and the diverse range of photocatalytic applications that have been explored within this domain.

Applications. In the past twenty years, interest upsurged in an innovative category of permeable materials, designated as MOFs, which have been used for extensive applications such as catalysis, photocatalysis, electrocatalysis, water splitting, supercapacitors, lithium-ion batteries, sensors, and drug delivery. MOFs' configuration comprises metal centers and organic bonds that amalgamate to generate boundless crystal networks. Composite structures that integrate organic and inorganic components have a promising versatility that enables them to be systematically classified into three distinct groups: 1) metal azolate frameworks, 2) metal carboxylate frameworks, and 3) MOFs with hydrophobic properties [95]. These compounds are renowned for their distinctive crystal structure, characterized by exceptional pore shape and size, impressive performance, thermal stability, surface area, and incredible flexibility. These remarkable properties give them extraordinary versatility and enable them to effectively remove various contaminants, including azo dyes, heavy oil, pharmaceuticals, and metal ions. Because of their significant influence in these domains, these composite structures have undergone extensive examination and analysis in environmental treatment and materials science. The ability to manipulate the undesirable properties of these structures enables the development of customized materials with enhanced

Table 2
Synthesis methods of some MOFs.

MOFs	Synthesis Method	Reaction Conditions: Solvent, Temperature (°C)	Reaction Time (h)	Ref.
MOF-5	Solvothermal	DMF, 130	12	[81]
HKUST-1	Solvothermal	DMF, 140	0.25	[82]
ELM-11	Reflux	Methanol, 70	15	[83]
MIL-47	Microwave	DI water, 175	0.5	[84]
MIL-53(Fe)	Hydrothermal	DMF, 150	72	[85]
MIL-88 (Fe)	Ultrasonic	DMF, 85	12	[86]
MIL-100 (Fe)	Hydrothermal	HF, 160	120	[87]
MIL-101(Cr)	Hydrothermal	HF, 200	8	[88]
MIL-100(Cr)	Hydrothermal	220	15	[89]
CPO-27-Ni	Reflux	THF, 67	24	[90]
UiO-66	Hydrothermal	DMF, 120	48	[91]
ZIF-8	Reflux	Methanol, 60	24	[92]
UTSA-16 (Zn)	Microwave	DI water & ethanol, 90	1–6	[93]

DMF = Dimethylformamide; HF = Hydrogen fluoride; THF = Tetrahydrofuran.

Advantage	Synthesis methods of MOFs	Disadvantage
<ul style="list-style-type: none"> • High degrees of crystallinity in the structure • The ability to tune the size and morphology 	Solvothermal/Hydrothermal	<ul style="list-style-type: none"> • Needs organic solvents • Requires long reaction times with high temperature and pressure
<ul style="list-style-type: none"> • A facile and rapid strategy • Synthesis methods 	Microwave	<ul style="list-style-type: none"> • Formation of a secondary phase
<ul style="list-style-type: none"> • Small nanocrystals • High degrees of crystallinity in structure 	Sonochemical	<ul style="list-style-type: none"> • Several external parameters can affect the yield of the process
<ul style="list-style-type: none"> • Possibility of synthesizing thin films 	Electrochemical	<ul style="list-style-type: none"> • The mechanism of growth is unknown yet
<ul style="list-style-type: none"> • Synthesis of pure MOF crystals, and MOF hybrid structures • Minimal amounts of solvents 	Mechanochemical	<ul style="list-style-type: none"> • Scale-up faces challenges Solvents may be still required for purification
<ul style="list-style-type: none"> • Different particles with controlled composition and morphology 	Microemulsion	<ul style="list-style-type: none"> • Low yield of product • Toxicity of solvents and surfactants

Fig. 2. Advantages and disadvantages of techniques used for synthesis of MOFs.

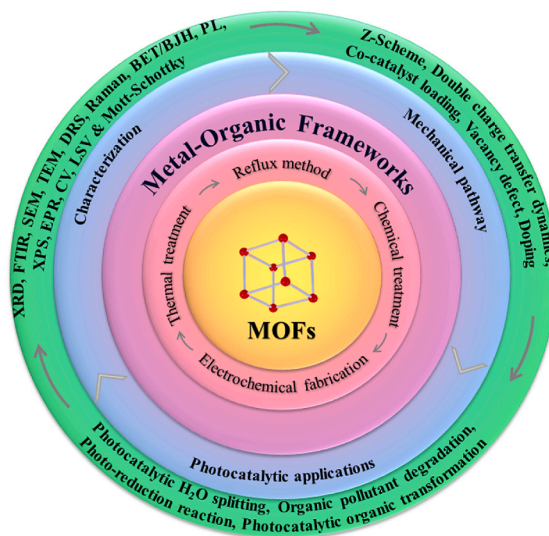


Fig. 3. Methods for synthesis, characterization, mechanical path, and applications of MOFs [88,94].

adsorption and catalytic properties, thus leading to promising advances in several applications such as water purification, gas separation, and drug delivery systems. Furthermore, the exceptional properties exhibited by these composite structures have aroused considerable interest in energy storage, as they have shown significant potential for integration into batteries, supercapacitors, and fuel cells [96]. Fig. 4 depicts the use of MOFs in various fields and industries and demonstrates their myriad applications.

As illustrated in Fig. 4, it is evident that MOFs possess many noteworthy applications, particularly in photocatalytic processes. Using photocatalytic decomposition for wastewater treatment surpasses alternative techniques such as filtration, coagulation, and adsorption. Using photocatalysts represents an efficient approach for wastewater treatment in which catalytic nanostructures are used, and light-emitting properties activate these nanostructures. As a result, these active catalyst nanostructures can eliminate various pollutants in wastewater. It is noteworthy that MOFs have organic bonds that provide them with a relatively broad absorption spectrum. This broad absorption spectrum is very important in influencing the degradation of pollutants in short time intervals [40].

Photocatalytic oxidation process. Water and wastewater treatment technologies (Fig. 5) use different physical processes, such as filtration, sedimentation, centrifugation, electrocoagulation, and advanced methods, such as membrane technology, biological treatment, surface adsorption, and advanced oxidation processes (AOPs) [97,98]. Among the various methods mentioned above, it is crucial to highlight the significance of the AOP approach, primarily because of its exceptional level of performance that surpasses other methodologies [99]. Recently, AOPs have been used as a suitable alternative to conventional purification processes due to their ease of use, economic aspect, and high efficiency. In AOPs, pure oxygen and ozone are injected into the wastewater at different stages. With



Fig. 4. Applications of MOFs [40].

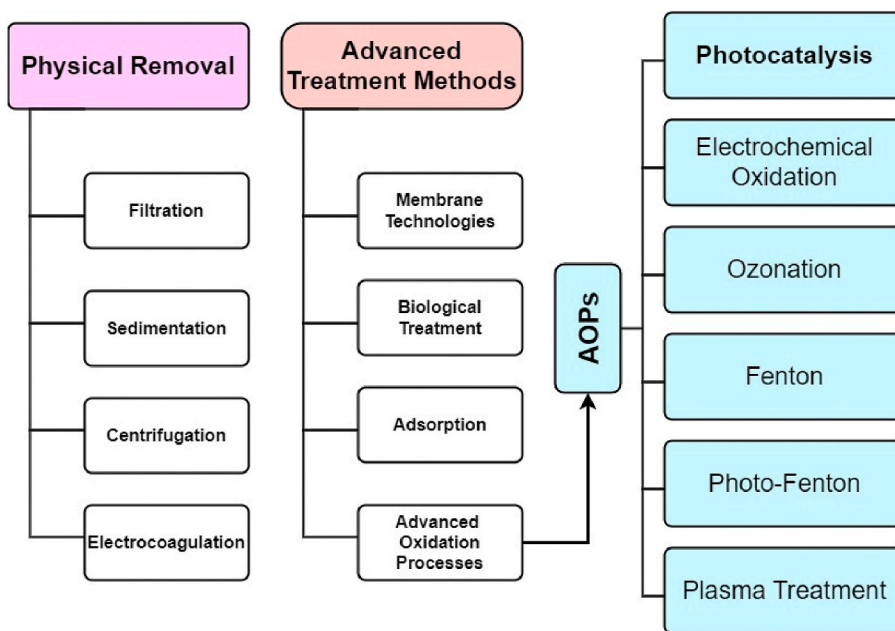


Fig. 5. Different approaches for wastewater treatment.

strong oxidizing properties, they degrade pollutants and purify the wastewater. Photocatalysis, electrochemical oxidation, ozonation, fenton, photo-fenton, and plasma treatment methods are based on AOPs. The advantage of the photocatalytic process over other AOPs is the ability to use sunlight to degrade pollutants and produce harmless final products such as H₂O and CO₂ [100].

MOFs photocatalysis in wastewater treatment. Worldwide, densely populated residential, commercial, and industrial centers develop around water sources such as rivers, lakes, and groundwater reservoirs. These sectors contaminate the water sources with large quantities of various types of effluents containing physical, chemical, and biological contaminants. Specifically, water resource contamination with anthropogenic chemical compounds from industrial effluents has provoked long-lasting concerns. The textile industry holds a significant position within the economic landscape of numerous countries. Due to the use of about 10,000 types of dyes, textile wastewater has always been a cause of concern for governments across the globe. The effluents of these industries contain a wide range of chemicals, mainly dangerous and non-biodegradable compounds. They have low biochemical oxygen demand (BOD) and high chemical oxygen demand (COD) [101]. It is important to acknowledge that the composition of this type of wastewater changes over time. As a result, there are many pigments, detergents, sulfide compounds, solvents, heavy metals, and mineral salts. One

of the major environmental pollutants in the effluents of various industries, including textiles, are dyes that cause pollution for humans and the environment. Most of the colors used in these industries are synthetic colors that, due to their toxicity and slow decomposition, can cause irreparable damage if they enter the environment without purification. Therefore, such wastes should be treated using appropriate methods before discharging into the environment [102]. A significant advancement has been achieved in the decomposition of organic dyes through the utilization of photocatalysts based on MOFs, resulting in an enhanced application of high-performance MOFs for the degradation of dye pollutants such as methylene blue (MB) [103], rhodamine B (RhB), and methyl orange (MO) [103]. However, it is important to highlight the fact that pharmaceutical compounds, which constitute a significant category of water pollutants, pose a critical challenge. This is primarily attributed to their wide variety, widespread consumption, and ecological impact on the environment [104]. These pollutants penetrate into the environment through various ways, such as pharmaceutical, hospital and household wastewater, and agricultural runoff resulting from waste disposal. Consequently, there is an urgent need to identify a safe and efficient mechanism for the degradation of pharmaceutical compounds. Considering this goal, photocatalysts based on MOFs as an emerging and new material are of considerable value for the degradation of pharmaceutical wastewater [105]. Unlike other types of semiconductors, MOFs have a diverse set of attractive surface properties that are not limited to the top surface. These properties also include regular porous structures and tunable functional groups, as highlighted in previous research studies [106]. Furthermore, it is important to emphasize that the MOF family includes many well-known members, including but not limited to the ZIF, UiO, and MIL series [107,108]. MOFs' incredible versatility and adaptability allow them to serve as a promising basis for developing innovative and highly efficient synthetic photosynthetic systems. Therefore, it is evident that MOFs have the potential to become an important substrate for the development of new and effective artificial photosynthesis. Energy transfer from organic junctions to metal-exo clusters typically occurs when these materials are exposed to light [109]. This phenomenon has been observed especially in some MOFs such as ZIF-67 and UiO-68. Nevertheless, it is important to note that the photocatalytic efficiency of most MOFs is relatively insufficient. This can be attributed to their limited capacity to harvest light efficiently and their wide BGs, which hinder the efficient use of light energy for photocatalytic methods [110]. Various approaches have been suggested and put into practice to improve MOFs' photocatalytic performance. Modifications to the inorganic components or molecular bonds are among the tactics employed to bolster the photocatalytic potential of MOFs. The primary aim of these adjustments is to significantly augment the capability of MOFs to facilitate photocatalytic reactions. These strategies have been proven effective in increasing the photocatalytic activity of MOFs, as reported in open sources [111]. As anticipated, utilizing modified MOFs as catalysts typically improves the performance of photocatalytic wastewater treatment. However, MOFs-based photocatalysts still have significant obstacles that should be overcome. The elimination of organic contaminants, metal ions, and microorganisms, all of which present considerable apprehensions in wastewater management, is an imperative that should not be disregarded [112]. It is worth noting that numerous studies have shown that most pristine MOFs exhibit poor photocatalytic performance. This low performance prevents the effective eradication of hazardous substances during wastewater treatment processes. It is important to highlight that the wide BGs that characterize most photocatalysts significantly hinder their ability to absorb sunlight, thereby limiting their overall efficiency. Consequently, these photocatalysts can only absorb UV light, which is a significant drawback. In addition, the problem of electron and hole recombination often arises in the internal and surface of photocatalysts and thus imposes significant limitations on their overall catalytic activity

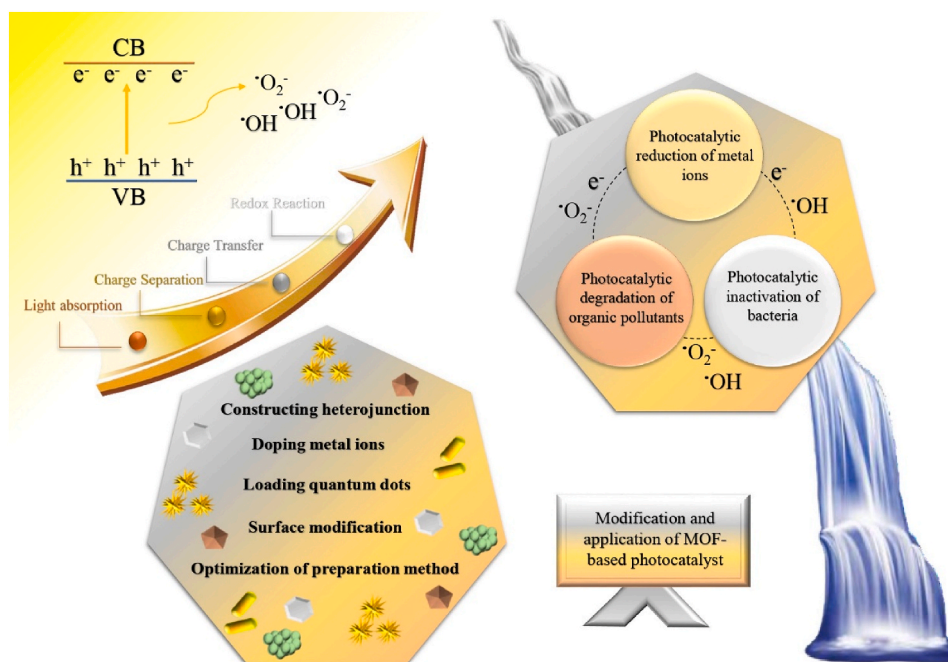


Fig. 6. Application of MOF photocatalysts modified in wastewater treatment [114].

[113]. These limitations should be considered when employing MOF-based photocatalysts for removing hazardous substances. When considering the configuration of photocatalysts with superior performance, we should focus on two main goals; namely, expanding the range of photocatalysts' light absorption capabilities and increasing the efficiency of separation and transfer of electron-hole pairs produced through the photoinduction process [114]. To achieve the above goals, researchers have designed and implemented several effective strategies to achieve desirable results [115]. As illustrated in Fig. 6, a variety of techniques can be used to enhance the performance of MOFs.

2.2. MOFs surface modification

MOFs exhibit a wide array of uses in the realm of industrial waste water treatment and water splitting. The distinguishing features of MOFs include a substantial surface area, high porosity, congenial chemical composition, adaptable structure, and varied functionalities. Nevertheless, notwithstanding their advantageous characteristics, the practical utilization of MOFs encounters certain constraints, notably including elevated production expenses, inadequate specificity, restricted capacity, and challenges pertaining to recovery and restoration. These concerns are tackled through methodologies such as the modification of surfaces [116].

Functionalization of MOFs: Previous studies show that when the surface of MOFs is modified, their adsorption performance is enhanced, thus increasing the overall efficiency and stability of MOFs as potential materials for various applications such as separation, treatment, and reactive processes [117]. Modifying the surface of MOF photocatalysts to enhance the adsorption of pollutants represents an alternative approach to augmenting photocatalytic activity, as this modification effectively reduces the lifespan of reactive oxygen species (ROS) generated during the process. To achieve the desired goal of increasing the photocatalytic activity of MOFs, a proper method involves the modification of organic ligands, which can be conducted by integrating functional units or incorporating foreign materials at the molecular level of MOFs. This approach is not only a means to increase the performance of MOFs, but also opens new ways to develop advanced materials with improved photocatalytic properties and potential applications in various fields, such as energy conversion and environmental cleanup. This approach enables the manipulation of ligand characteristics/features, significantly increasing the overall photocatalytic activity of MOFs. Incorporating functional units into organic ligands brings additional functionalities and structural changes, thereby enhancing the light absorption capacity and enhancing charge separation in MOFs [118]. Several functional units that are commonly used in various synthetic methods are amino group (-NH₂), hydroxyl group (-OH), bromine atom (-Br), chlorine atom (-Cl), and thiol group (-SH) [119]. The successful synthesis of UiO-66-NH₂, a modified variant of UiO-66, was reported by Silva et al. [120]. This was achieved using a thermal solvent method. The strategic incorporation of amino substituents into the UiO-66-NH₂ framework gives it the unique advantage of having exochromic and bathochromic functionalities. As a result, UiO-66-NH₂ demonstrates a significantly improved VIS light adsorption capacity compared to UiO-66. This significant increase in light absorption has resulted in superior photocatalytic efficiency of UiO-66-NH₂ in the H₂ production process [121].

MOFs doping metal ions. The improvement of photocatalytic properties of MOFs using metal doping has been well documented in various studies conducted in the past [122–124]. Introducing metal ions into the photocatalyst material allows these ions to act as electron absorption centers in the photocatalyst. This unique role enables the facilitation of electron transfer processes and ultimately leads to the formation of an optical hole [125]. Furthermore, it is important to consider that metal ions, when added to the photocatalyst, can produce an impurity surface in the BG of the photocatalyst, thereby leading to an increase in the extent and range of light absorption. Additionally, incorporating different metal ions can create network defects capable of generating active centers. Consequently, it is common to use transition metals (Fe³⁺, Co²⁺, and Ni²⁺) as well as rare earth metals (Er³⁺, Ce³⁺, and La³⁺) as metal ions [126]. In the contemporary era, research investigations regarding doping transition metals in MOFs to alter photocatalytic activity have caused increased interest due to the benefits of ease and efficacy. Transition metals into MOFs can generally be incorporated by utilizing a straightforward one-pot technique; whereby metal ions are introduced to replace partial metal centers within the MOFs [127].

MOFs loading quantum dots. Loading quantum dots (QDs) into the MOFs matrix is a distinct process compared to the previously discussed surface modification. In particular, loading QDs requires encapsulating the QDs in the MOF matrix. The process involves using a bottle-around-the-ship approach where QDs are first synthesized and subsequently, MOF precursors are assembled around the QDs to form the composites [128]. To demonstrate this method, a study used the vessel technique to synthesize QDs decorated with Fe-based MOFs in a surrounding bottle [129]. It was found that introducing CdSe QDs into Fe-based MOFs led to changes in the BS of MOFs and reduced the BG. In conclusion, the decorated Fe-based MOFs showed photocatalytic degradation ability for RhB under VIS light. This observation highlights the potential of using CdSe QDs-loaded MOFs for efficient VIS light-driven photocatalysis. However, there are other methods available for combining MOFs and QDs, such as the preparation of boron nitride (BN) QDs and MIL-100(Fe), as described by Wang et al. [130]. Then, the combination of BN QDs and MIL-100 (Fe) in an ethanol solvent was performed with the intention of enhancing the photocatalytic degradation of antibiotics. This mixture was sonicated using an ultrasonic technique. The composites that were obtained demonstrated outstanding performance, a result that can be credited to the effective integration of BN QDs within the MIL-100 (Fe) framework. Thus, it can be concluded that incorporating QDs into matrix MOFs represents a very suitable approach to increasing the activity and efficiency of photocatalysis. Various efficient materials are currently used to develop and create heterojunctions with MOFs. Some notable examples are TiO₂, CdS, g-C₃N₄, COFs, Bi₂O₃, Bi₅O₇I, and Fe₂O₃. Using heterojunction connections leads to a significant increase in charge transfer efficiency in photocatalysts. This improvement can be attributed to the potential difference in the heterojunction, which creates favorable conditions for transferring charges and facilitates their efficient transfer from one component to another [131].

Z-scheme heterojunction. The position of the BS is the same in Z-scheme and heterojunction system, while the path and method of

charge transfer differ. The Z-scheme process, which finds its inspiration from the complex and fascinating process of natural photosynthesis, is a synthetic approach that has attracted considerable attention in photocatalysis. This effective method cleverly integrates two separate semiconductors with unique properties and functions [132,133]. One semiconductor assumes the responsibility of an oxidizing agent and thus facilitates the oxidation process. At the same time, the other semiconductor takes the role of a reducing agent that reduces some substances by donating electrons. This coordinated interaction between the two semiconductors leads to a synergistic effect and activates the desired chemical reactions. It is worth noting that the oxidation ability of the photocatalyst is directly affected by the VB energy level, and a lower VB results in a stronger oxidation capacity. Meanwhile, the photocatalytic reduction

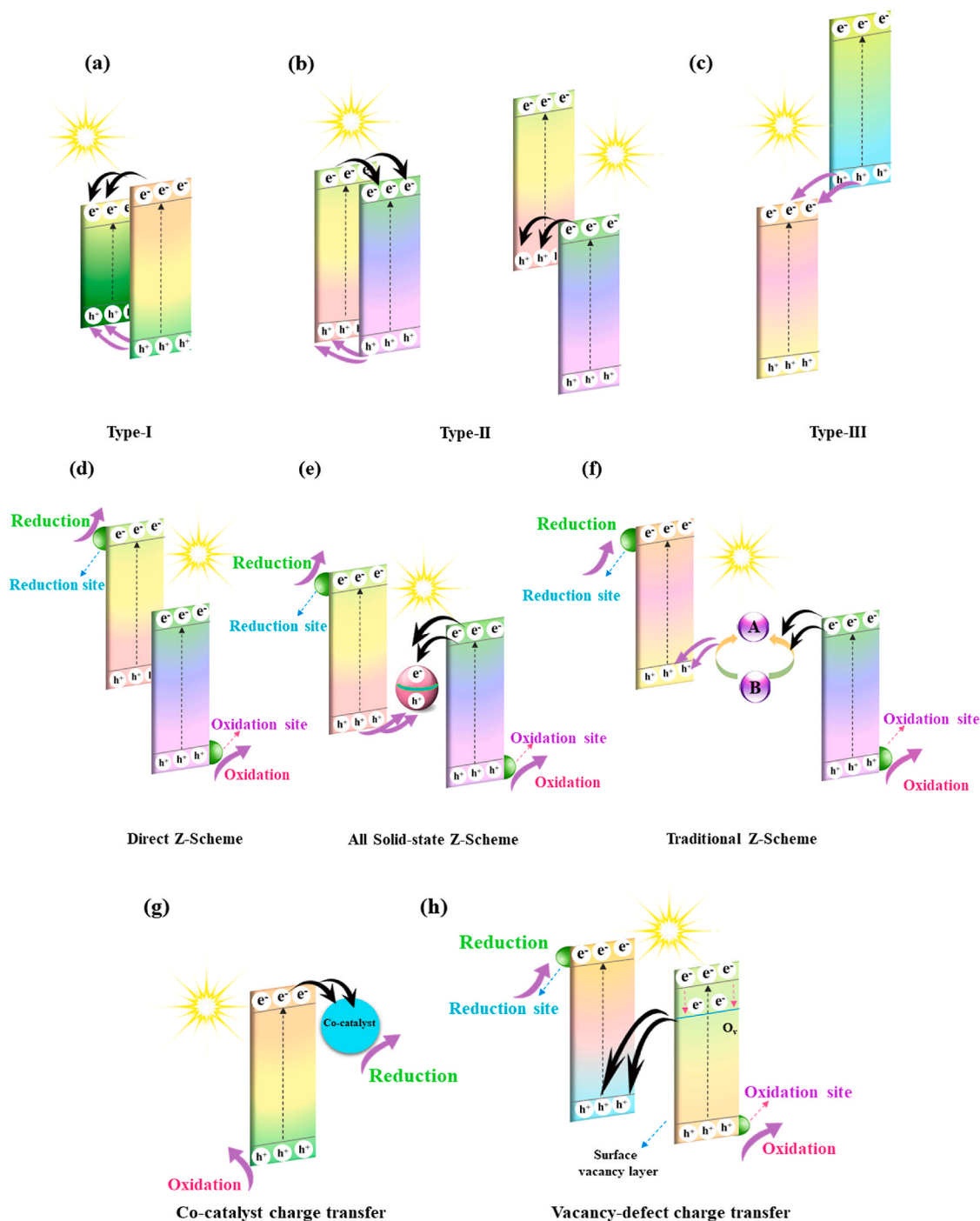


Fig. 7. Different types of configurations of heterojunction-based charge dynamics: a) type-I, b) type-II, c) type-III, d) direct Z-scheme, e) all solid-state Z-scheme, f) traditional Z-scheme, g) Co-catalyst charge transfer, and h) mechanism of vacancy-defect charge transfer [134].

occurs in the location of the higher CB. Z-scheme photocatalysts can be categorized into three groups based on the type of mediating charge carriers: traditional photocatalysts that use ions as charge transfer media reserves, all solid-state photocatalysts that employ electron conductors for easy transfer, and photocatalysts with direct contact between semiconductors created by an internal electric field as a stimulus for charge carrier transfer. Utilizing heterojunction between two semiconductors has the advantage of actively separating electrons from holes, consequently suppressing charge recombination [134]. Characterized by various features and behaviors, heterojunctions are usually divided into three distinct categories: Type-I, type-II, and type-III, as presented visually in Fig. 7 (a–c). A key strategy used to increase photocatalytic activity efficiency involves using metal catalysts on the surface of semiconductors [135]. The main purpose of using photocatalysts revolves around the excitation of electrons through the medium of light [136]. Fig. 7 (c) clearly illustrates the nature of this phenomenon by providing a comprehensive picture of this complex process. Co-catalysts commonly used in semiconductors mainly comprise noble metals such as gold, platinum, palladium, and rhodium. In addition, these catalysts include transition metals and their corresponding oxides, as well as metal sulfides and metal phosphates, and have relatively lower Fermi energy levels than semiconductors. Consequently, when light interacts with the photocatalytic surface of the host material, the resulting electrons are trapped due to this energy difference. Including a co-catalyst not only diminishes the surplus potential but also assumes a significant function in augmenting the division between electrons and holes stimulated by the incoming light. Consequently, it becomes a vital element in advancing the photocatalytic efficiency in semiconductors [134].

A mechanism called Z-scheme is designed to increase the movement of charges using photoexcitation process in two separate semiconductors, Photosystem I, and Photosystem II (PS I), and (PS II), which have different BGs. The fundamental principle underlying the Z-scheme primarily revolves around the association of light-excited electrons in the CB of one semiconductor, which interacts with light-excited holes in the VB of another semiconductor through a phase transition in the interface. This process is characterized by an oscillatory behavior in which electrons move back and forth between the two semiconductors [136]. In the Z-scheme presented in Fig. 7(f), an additional step is implemented in the liquid phase to effectively enable the sequential progression of events, thereby creating a mechanism that requires direct physical interaction between the two optical systems. This intermediate step, which acts as an intermediate component in the complex framework of the photosynthesis process, plays an important role in facilitating the seamless and highly efficient transfer of excited electrons from PS II to PS I. Introducing this intermediate step not only increases the overall efficiency of the Z-scheme, but also allows for a controlled and regulated flow of electrons, thereby maximizing the energy conversion process. It is important to note that the role of redox mediators in promoting charge transport is very important. For excitons to conduct properly, it becomes necessary that PS I electrons are consumed by species acting as electron acceptors, while PS II holes are consumed by species acting as electron donors. The solid-state Z-scheme, illustrated in Fig. 7(e), relies heavily on selecting an appropriate solid conductor for effective electron trapping. Incorporating a conductor is necessary to form an ohmic contact between two photosystems, with Au, Ag, Pd, Cu, and other similar materials serving as mediators for photo-excited electron channelization [134]. The electron trapping capabilities of all solid-state Z-schemes make them more efficient than their liquid-phase counterparts. Direct Z-schemes, as depicted in Fig. 7(d), are even more effective in proper exciton channelization when compared to the methods mentioned above. The extended lifetime for the active species is a consequence of the absence of a redox mediator that acts as a catalyst in facilitating redox reactions [134].

The defects observed in MOFs are intrinsically related to the displacement of atoms or ions within the structure, hence hindering the pristine periodic arrangement of the framework, ultimately leading to the appearance of structural defects. These defects, which appear in various forms, can be classified according to their dimensional characteristics, including point, line, planar, and volume defects [137]. In MOFs, the fundamental importance of point defects and extended defects should be acknowledged. A point defect is caused by the presence of a vacancy in the core of the metal or organic ligand, which may result in the absence of a defective anion or

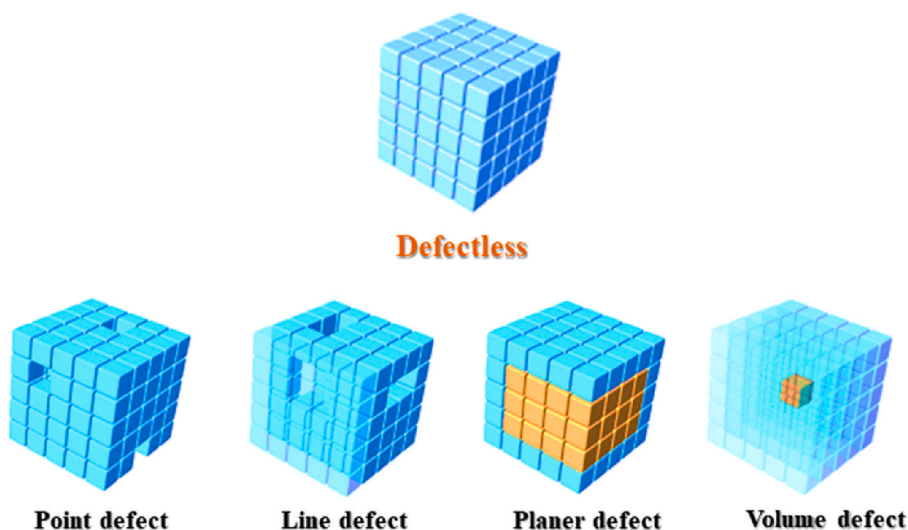


Fig. 8. Various types of defects in MOFs.

ligand, as well as the absence of a cation. Extended defects are responsible for 1D/2D defects in the crystal structure. The inclusion of defects in MOFs can occur through two methods: during MOF synthesis or post-synthetic modification. The various categories of defects are illustrated in Fig. 8.

The latter technique can produce numerous active defective sites that improve the MOF's functionality. Vacancy incorporation can overcome the recombination process in MOFs. The presence of vacancy defects can control the performance of photocatalytic reactions [138]. These defects play a fundamental and vital role in significantly increasing the capacity of photocatalysis. Hence, they contribute to a phenomenon that has attracted considerable attention and interest in various scientific circles. An accurate and comprehensive evaluation and measurement of this remarkable and fascinating phenomenon can be achieved through careful examination of three basic mechanisms: light absorption capacity, efficiency in separation of charge carriers, and ability to participate actively in surface reactions in a dynamic manner. An in-depth analysis/insight into these mechanisms is clearly illustrated in Fig. 7(d), which aids in understanding the complexities of this phenomenon. In addition, this phenomenon leads to the energy difference between the capacitance and CBs, which provides researchers and scientists with a promising and unique opportunity to modify and adjust the properties of materials with their desired and required characteristics, which include transfer. The phase becomes magnetic and ferroelectric. Also, this reduction of the distance between the bands facilitates and enhances the unprecedented and significant expansion and enhancement of the optical response range. As a result, the above phenomenon leads to a significant improvement in the optical properties of the photocatalyst, which positively affects its overall performance [134].

MOFs Z-scheme heterojunction. In semiconductors, it is important to note that the concentration of electrons or holes is significantly lower than that found in solutions. As a result of this phenomenon, the difference between the two previously mentioned conditions causes a spatial redistribution of electric charges within an electrode made of a semiconducting material although in a spatial range significantly larger than that usually observed happening in liquid solutions. This redistribution of space charge is ultimately responsible for the appearance of potential bending on the surface due to the redistribution of charge in the conductive and capacitive band [139,140]. When analyzing the electrode made of n-type semiconductor in the non-closed state, a particularly noteworthy observation is that the Fermi level exceeds the redox potential of the electrolyte. As a result, an attractive phenomenon occurs whereby the electrons residing in the electrode are effectively transferred into the solution, manifesting a positive charge that occupies the space charge region. This event, in turn, causes the band edge of the capacitor to bend, a phenomenon commonly called edge voltage bending (E_{VB}) [141]. On the other hand, when dealing with p-type semiconductors, the opposite effect is observed, where the band edges point downward. It is important to emphasize that the degree and direction of this bending phenomenon depend on the applied potential [142]. Indeed, no bending occurs at a given applied potential, and this particular potential is referred to as the flat band potential, denoted as E_{fb} . Electrochemical methods, especially Mott-Schottky diagrams, can be very useful in determining this potential's magnitude. When considering the properties of Z-scheme heterojunction structures, it becomes important to emphasize its role in facilitating electron momentum transfer, leading to high conductivity and spontaneous electron transfer over the heterojunction Mott-Schottky. Using these electrochemical techniques and analysis of Mott-Schottky diagrams, one can gain valuable insight into system behavior and understand the mechanisms behind electron transfer and electron conduction in Z-scheme heterojunction structures [143]. In these special structures, when one of the components enters an excited state, the electrons it produces begin to flow to the other component [144]. In those structures where electron transport follows a path known as the Mott-Schottky path, the Z-scheme is observed to provide significant confirmation in the form of strong signals consisting of both electrons and holes. The

Table 3
Summary of Mott-Schottky Z-scheme structures, BGs, types, and E_{VB} .

MOFs-Z scheme	BG (eV)	Type	E_{VB} (eV)	Ref.
ZIF67/WO ₃	ZIF67 = 1.98	ZIF67 (n)	ZIF67 = 2.167	[146]
UiO-66/NH ₂ -MIL-125/g-C ₃ N ₄	WO ₃ = 2.98	WO ₃ (n)	WO ₃ = 3.33	[147] [148]
In ₂ S ₃ @PCN-224	g-C ₃ N ₄ = + 1.60	g-C ₃ N ₄ (n)	g-C ₃ N ₄ = -1.08	[149] [150]
NH ₂ -MIL 125(Ti)/CdS	NH ₂ -MIL-125 = + 3.17	NH ₂ -MIL-125(n)	NH ₂ -MIL-125 = -0.31	[151]
Bi ₂ SeO ₅ /rGO/MIL-88A	UiO-66 = + 3.22	UiO-66(n)	UiO-66 = -0.6	[152]
Bi ₂ WO ₆ /NH ₂ -UiO-66	In ₂ S ₃ = 2.24	In ₂ S ₃ (n)	In ₂ S ₃ = 1.92	[153]
BiFeO ₃ /UiO-66	PCN-224 = 1.78	PCN-224 (n)	PCN-224 = 1.25	[154]
UiO-66-NH ₂ /PhC ₂ Cu	NH ₂ -MIL 125(Ti) = 2.35	NH ₂ -MIL 125(Ti) (n)	NH ₂ -MIL 125(Ti) = 2.2	[155]
Bi ₄ O ₅ Br ₂ /MIL-88B(Fe)	CdS = 2	CdS (n)	CdS = 1.45	
Carbon nitride/NH ₂ -MIL-53 (Fe)	Bi ₂ SeO ₅ = 3.53	Bi ₂ SeO ₅ (n)	Bi ₂ SeO ₅ = 3.49	
	MIL-88A = 2.83	MIL-88A(n)	MIL-88A = 2.25	
	Bi ₂ WO ₆ = 2.82	Bi ₂ WO ₆ (n)	Bi ₂ WO ₆ = 2.16	
	NH ₂ -UiO-66 = 2.86	NH ₂ -UiO-66 (n)	NH ₂ -UiO-66 = 2.36	
	BiFeO ₃ = 2	BiFeO ₃ (p)	BiFeO ₃ = 2.63	
	UiO-66 = 3.5	UiO-66(n)	UiO-66 = 2.90	
	UiO-66-NH ₂ = 3.03	UiO-66-NH ₂ (n)	UiO-66-NH ₂ = 2.15	
	PhC ₂ Cu = 2.59	PhC ₂ Cu=(p)	PhC ₂ Cu = -2.19	
	Bi ₄ O ₅ Br ₂ = 2.56	Bi ₄ O ₅ Br ₂ (n)	Bi ₄ O ₅ Br ₂ = 2.06	
	MIL-88B(Fe) = 2.24	MIL-88B(Fe)(n)	MIL-88B(Fe) = 2.27	
	Bi ₄ O ₅ Br ₂ /MIL-88B(Fe) = 2.27	Bi ₄ O ₅ Br ₂ /MIL-88B(Fe)(n-n)	Carbon nitride = 1.53	
	Carbon nitride = 2.05	Carbon nitride (p)	NH ₂ -MIL-53(Fe) =	
	NH ₂ -MIL-53(Fe) = 2.45	NH ₂ -MIL-53(Fe) (n)	2.32	
	carbon nitride/NH ₂ -MIL-53(Fe) = 2.31	Carbon nitride/NH ₂ -MIL-53(Fe) (p-n)		

signals detected in the empirical evidence can be ascribed to the increased spatial differentiation that arises amidst the electron-hole pairs. This increase in spatial separation between electron-hole pairs is responsible for the manifestation of these signals. As a result, it can be concluded that Mott-Schottky heterojunctions, which have an additional level of Z-scheme heterojunction, show a high ability for molecular activation and a superior performance level compared to other structures such as $g\text{-C}_3\text{N}_4$, metal oxides, and metal sulfides [145].

Accurately predicting the mechanistic pathway of charge dynamics in photocatalysts is of great importance, particularly in the context of MOFs Z-scheme heterojunction, as they may give rise to any one of a range of mechanistic pathways. In this regard, a comprehensive understanding of the science of exciton generation, channelization, and recombination is crucial [145]. Table 3 summarizes Mott-Schottky Z-scheme structures, BGs, types, and E_{VB} .

In the realm of water splitting, an imperative factor to consider is the significant amplification in the speed at which H_2 generation occurs, so as to effectively meet the demands of industrial manufacturing. In order to surmount these challenges, the establishment of architectures of MOF Z-scheme, which possess a commendable potential for photoreduction, an exceedingly efficient process of charge separation, and the ability to enhance mutual light absorption, will undoubtedly prove to be an invaluable asset in the creation of sophisticated photocatalytic systems. As such, this will greatly facilitate the efficient and selective evolution of H_2 [156–158].

3. MOFs Z-scheme heterojunction for wastewater treatment

He et al. [159] studied heterojunction MOF/COF with direct Z-scheme. In particular, the researchers focused on investigating direct heterojunction coupling between a MOF and a COF that had a Z-scheme structure; the created structure exhibited improved photocatalytic activity under VIS light. They have developed a series of new MOF/COF hybrid materials through a MOF coating process with 4,4',4''-(1,3,5-triazine-2,4,6-triyl) tribenzaldehyde (TTB)/4,4',4''-(1,3,5-triazine-2,4,6-triyl) trianiline (TTA) (TTB-TTA); a remarkably stable COF was synthesized from TTB and TTA. This unique coating technique allowed the hybrid materials to retain their optimal properties, such as exceptional response to VIS light, high crystallinity, large surface area, and tunable BG [159]. Furthermore, MIL-125- NH_2 facilitates optical, electronic, and redox properties, thereby enabling fine-tuning of these properties. The enhancement of photocatalytic degradation of organic pollutants has been significantly boosted by promoting diverse connectivity facilitated by its role in increasing charge separation. This has led to significant improvements in the efficiency and effectiveness of these compounds in removing harmful substances from the environment [160]. The photodegradation rate for MO in the MIL-125- NH_2 /TTB-TTA composite was considerably higher compared to pure MIL-125- NH_2 and TTB-TTA, indicating the versatility of the molecular material platform in achieving dual tuning states through molecular engineering and screening strategies [160].

Cheng et al. [161] examined using B/Ni-MOF sheets coated with Bi_2WO_6 to improve photocatalytic performance via direct electron transfer in the MOF Z-scheme. By successfully incorporating the compound Bi_2WO_6 onto two-dimensional nickel-based metal-organic framework (Ni-MOF) sheets, the researchers were able to create a groundbreaking and highly effective structure known as B/Ni-MOF. This innovative structure exhibited exceptional performance in the process of photocatalysis, specifically in the degradation of methylene blue (MB) using VIS light. The enhanced photocatalytic efficiency results from creating a heterojunction configuration, which directly links Ni-MOF and Bi_2WO_6 through a Z-scheme, thereby promoting the separation of light-induced charge carrier [160].

Wu et al. [162] investigated the utilization of a Z-Scheme ZIF-67/ BiOCl heterojunction to degrade organic dyes and antibiotics through photodegradation effectively. They employed ZIF-67 and BiOCl to construct MOF-based heterojunction structures to attain this feature. Indeed, these structures achieved an impressive 97.4% degradation of RhB and a commendable 78.2% degradation of TC exposed to VIS light. Additionally, cyclic experiments were performed, which revealed that after undergoing 4 cycles, 15% of the ZIF-67/ BiOCl remained structurally stable. Moreover, the trapping of active species during the degradation process indicated that the presence of $^1\text{O}_2$ and $\cdot\text{O}_2^-$ plays a significant role in the degradation of both RhB and TC. Furthermore, this groundbreaking work shed light on the degradation pathway and heterojunction mechanism, thereby providing valuable insights into synthesizing superior photocatalysts that can be utilized for environmental remediation [162].

Pan et al. [163] have successfully developed a modified $g\text{-C}_3\text{N}_4$ (MCN) heterojunction showing a highly effective Fe-MOF@ BiOBr Z-scheme for the degradation of ciprofloxacin (CIP). Achieving this remarkable photocatalytic performance was possible by synthesizing a new Fe-MOF@ BiOBr /MCN photocatalyst using a thermal solvent heating process with the help of ethylene glycol. Several methods were employed to thoroughly examine the properties, morphology, microstructure, and composition of photocatalysts. Importantly, the Fe-MOF@ BiOBr /MCN photocatalyst demonstrated markedly superior abilities in terms of pollutant adsorption and degradation compared to the pure BiOBr . The proper integration of Fe-MOF species and MCN is highly efficient in enhancing the overall system performance. Through the surface charge transfer process, the electrons generated by BiOBr were effectively transferred to both MCN and Fe-MOF species. This complex electron transfer mechanism significantly improved the separation efficiency of electrons (e^-) and holes (h^+). As a result, the overall effectiveness of the system increased significantly. It is worth noting that Fe-MOF@ BiOBr /MCN-50 showed a remarkable VIS light degradation rate of approximately 93% for CIP after 120 min of treatment. This rate of degradation is approximately 8 times greater than that of pure $g\text{-C}_3\text{N}_4$ and 1.5 times greater than BiOBr . The degradation process was ascertained to be driven by the primary reactive species through radicalization experiments and electron spin resonance (ESR) analysis, which revealed the existence of h^+ and $\cdot\text{O}_2^-$. Confirmation of the heterogeneity between MCN and BiOBr in the Z scheme was successfully achieved using DFT calculations and radical trapping experiments. The role of the Fe-MOF species in electron transfer is crucial for detailed understanding the complex process of photocatalytic degradation of water pollutants [162].

Using the well-known and applied concept of symbiotic relationships commonly observed in nature, Chai et al. [163] successfully designed and fabricated a highly innovative and unique adsorbent known as ZIF-8/sodium alginate-kappa-carrageenan (SC). The adsorbent was meticulously prepared through the utilization of a methodology referred to as phase inversion, which relies on the

in-situ one-pot method. This process involved the complex assembly of nanoscale ZIF-8 with polysaccharide matrices, forming highly efficient and effective ZIF-8/SC adsorbents. It is worth noting that this new adsorbent has exceptional mechanical performance and stability. A notable feature of ZIF-8/SC adsorption is its uniform distribution and surface consistency, which directly contributed to its outstanding 2887 mg/g adsorption capacity. It should be noted that this adsorption capacity exceeds most other adsorbents based on MOF or natural polymers. Moreover, the adsorption behavior shown by ZIF-8/SC adheres to the second-order isotherm and Langmuir models, thus indicating its robust and reliable performance in different adsorption scenarios. Based on these promising achievements, the researchers also synthesized a ZIF-8/SC column that served as an effective tool for dynamic separation. The findings from the experiments shed light on the complex and multifaceted dynamics that guide the absorption process. Several factors were shown to have a significant effect on the absorption process, thus highlighting the important role they play. These vital factors include the impact of electrostatic forces, the accumulation of π - π interactions, the interactions formed through hydrogen bonds, and the coordination effects between the adsorbent and the target compound. These findings underscore the complexity and subtle nature of the assimilation process, while simultaneously highlighting the critical importance of understanding and exploiting the various forces and interactions present. Such insights are valuable as they pave the way for further improvements and refinements in adsorbent development and utilization. Therefore, it can be concluded that the pioneering research conducted by Chai et al. [163] represents a significant milestone in adsorbent design and application and holds great promise for a wide range of industrial and environmental applications.

Spharmanhuri et al. [164] have fabricated a heterojunction consisting of a dual MOF/MOF Z-scheme, which shows significant efficiency in the photocatalytic degradation of ofloxacin (OFL). They performed an innovative study that developed a new species Z-scheme UiO-66/MIL-125-NH₂/g-C₃N₄ for degrading antibiotic OFL upon exposure to VIS light. The results obtained from the heterogeneity analysis provide convincing evidence to support the hypothesis that a dual Z scheme in this particular photocatalyst remarkably increases its efficiency as a catalyst for degradation of OFL. Furthermore, the important role of \cdot OH and \cdot O₂⁻ species in the photodegradation of OFL has been proven through radical trapping and EPR findings.

Mu et al. [165] have developed an innovative photocatalyst using the hydrothermal method to construct a 3D hierarchical structure. This structure comprises UiO-66-(COOH)₂ nanoparticles (NPs), and MoS₂ nanoplates, which are intricately decorated in the petal nanoplates connected to ZnIn₂S₄ microspheres. The fabrication process forms various crosslinks with many catalytic active sites and facilitates close interaction between the surfaces. In addition, integrating the charge transfer mechanism into the Z-scheme substantially enhances the oxidizability and reducibility of the photocatalyst, thereby influencing a highly significant and indispensable contribution to the overall advancement of the photocatalytic reaction, which in turn holds huge potential for different applications in the realm of sustainable energy conversion and environmental remediation. To optimize UiO-66-(COOH)₂/MoS₂/ZnIn₂S₄ photocatalyst, Mu et al. [165] conducted a series of designed experiments. These experimental efforts demonstrated the high capabilities of the photocatalyst in terms of H₂ production and photocatalytic reduction of Cr(VI) when exposed to simulated solar radiation.

Chang et al. [166] have provided evidence for the existence of Z-scheme heterojunction by incorporating Ag/AgCl into porous Co₃O₄ (C400) material obtained from the thermal decomposition of ZIF 67 to facilitate photocatalysis under VIS light irradiation. The successful incorporation of Ag/AgCl into porous CO₃O₄ at 400 °C can be attributed to the conductive potential and the suitable valence coupling exhibited by C400 and Ag/AgCl. Due to these features, the production of superoxide (\cdot O₂⁻) and hydroxyl radical (\cdot OH) is facilitated, which leads to an increase in the light oxidation reaction. The enhanced catalytic performance and effectiveness of Ag/AgCl/C400 can be attributed to the increased photoresponse and improved separation of photocarriers resulting from incorporating Ag/AgCl into C400 [166].

Chang and co-workers [167] have successfully synthesized a heterojunction known as Z-scheme AgCl/Ag-ZIF-8 through a well-defined and precise two-step process, as documented in their published work. Optimization of ion doping in the ZIF-8 framework, especially Ag cation in the imidazole ring, along with AgCl deposition, has led to a significant increase in the light-harvesting ability of the photocatalyst by reducing the BG energy. The significance of this outcome holds substantial value in the field of photocatalysis due to its direct contribution towards the enhancement of the overall efficacy of the photocatalysis process. In addition, the formation of AgCl/Ag-ZIF-8 stitched separation in the Z-scheme has been proven to improve the separation efficiency. Light-induced carriers are very beneficial. This finding has been confirmed through detailed photoelectrochemical experiments. The identification carries important consequences as it confirms the effectiveness of the synthesis procedure and highlights the outstanding efficiency of the AgCl/Ag-ZIF-8 photocatalyst in the presence of VIS light. The enhanced photoreaction capability of this innovative substance has the potential to revolutionize the realm of photocatalysis and generate prospects for exceptionally productive and environmentally friendly energy conversion approaches [167].

Ren et al. [168] effectively synthesized g-C₃N₄/UiO-66-NH₂ (CU) heterojunction photocatalysts through solvothermal and in situ methods. The resulting photocatalysts were exceptionally effective in the removal of Cr(VI) and showed the photocatalytic reduction of Cr(VI) and the oxidation of tetracycline hydrochloride (TC-HCl) in a systematic manner. The heterojunction structure composed of Cu-20% exhibited a removal efficiency for Cr(VI) that was 1.86 times greater than UiO-66-NH₂ under VIS light, as confirmed by both experimental and theoretical analyses [168]. Moreover, the prepared photocatalysts showed remarkable stability and reproducibility. The influences of two parameters, such as the concentration of Cr(VI) and the pH value, were extensively studied with regards to their impact on the photocatalytic efficacy of CU-20%. According to this research, it can be assumed that implementing photocatalysts with heterojunction bond structures is an efficient method for wastewater treatment. Based on the analysis performed in their study, a logical explanation is proposed for the reduction of Cr(VI) and oxidation of TC-HCl in the CU system when exposed to VIS light. g-C₃N₄ and UiO-66-NH₂ particles generate electrons and holes upon excitation by VIS light, which subsequently undergo transfer and intercombination. Finally, this process leads to the adsorption and removal of Cr(VI) and TC-HCl on the surface of the particles and

makes them effective photocatalysts. The detailed schematic of this mechanism can be seen in Fig. 9 [168].

Zhang and colleagues [169] were able to effectively create a Z-Scheme $\text{Bi}_2\text{WO}_6/\text{UiO}-66\text{-NH}_2$ heterojunction through the utilization of a two-step thermal solution method. The structure and composition of the composite material were comprehensively examined through the application of several analytical methods, such as XRD, FT-IR, and XPS, thus providing a systematic insight into its characteristics. In addition, the composite morphology was elucidated by SEM and TEM techniques. This comprehensive analysis allowed a detailed comparison of the photocatalytic activity of heterojunction composite materials with individual materials. In the end, it proved that the fabrication of heterojunction composite materials is more effective in separating photogenerated electron-hole pairs and it effectively increases the photocatalytic. It should be noted that the composite materials consisting of $\text{Bi}_2\text{WO}_6/\text{UiO}-66\text{-NH}_2$ displayed the maximum level of photocatalytic activity for removing RhB and TC pollutants. Furthermore, the exceptional performance of this composite was verified through a rigorous 4-cycle test, successfully demonstrating its inherent stability and exceptional reusability. To gain a deeper understanding of the fundamental mechanisms that determine the photocatalytic degradation process, the researchers performed a series of free radical trapping experiments. The findings of these experiments demonstrated the significance of $\cdot\text{O}_2^-$ and holes (h^+) as principal reactive agents that perform a crucial function in photocatalytic degradation. This discovery is important because it provides a detailed understanding of the fundamental processes and species involved in converting light energy into chemical energy. Recent research has also witnessed the extensive discovery of other photocatalysts, such as PCN-222 [170], ZIF-67 [171], MIL-88 A [172], and MIL-53 [173], which have shown exceptional efficiency and performance in modifying their various classes. A summary of these innovative photocatalysts can be found in Table 4.

According to the findings presented in Tables 4 and it is evident that the hydrothermal technique is the predominant method employed in the synthesis of Z-scheme heterojunction MOFs. The fabrication of Z-scheme heterojunction MOFs photocatalysts via hydrothermal and solvothermal routes exhibits superior efficiency, controllability, and biocompatibility.

4. MOFs Z-scheme heterojunction for water splitting

Dai et al. [195], presented a novel $\text{ZnCo}_2\text{S}_4/\text{MOF}-199$ (ZCS/M) photocatalyst, which operated through a direct Z-Scheme mechanism and was synthesized using an ultrasonic impregnation method with MOF-199 serving as the supporting material. This photocatalyst exhibited excellent efficiency and stability in the evolution of H_2 under simulated sunlight conditions. The ZCS/M photocatalyst showcased a notably heightened level of effectiveness in comparison to both MOF-199, and ZCS. The rate at which H_2 evolves has been determined to be 48, and 83 times higher, respectively. This significant increase can be attributed to the enhanced separation of electron-hole pairs, which is made possible through the direct Z-Scheme heterojunction.

Tripathy and colleagues [196] have effectively synthesized a composite material comprising of MgIn_2S_4 and $\text{UiO}-66\text{-NH}_2$ via a solvothermal technique. The composite material showcased remarkable efficacy in the production of H_2 and oxygen (O_2) by means of water splitting, surpassing the unaltered manifestations of MgIn_2S_4 , and $\text{UiO}-66\text{-NH}_2$. The improved efficacy observed in their study is ascribed to the successful interplay between the two constituents, which is facilitated by the transfer of electrons from $\text{UiO}-66\text{-NH}_2$ to MgIn_2S_4 . In addition, the composite exhibits an exceptional ability to segregate charges, further contributing to its enhanced performance. Their research serves as a valuable framework for the advancement of durable $\text{UiO}-66\text{-NH}_2$ based nanocomposite photocatalysts that effectively facilitate water redox reactions.

Xing and colleagues [197] were able to synthesize novel composites by combining a robust Zr-MOF and cost-effective $\text{g}-\text{C}_3\text{N}_4$

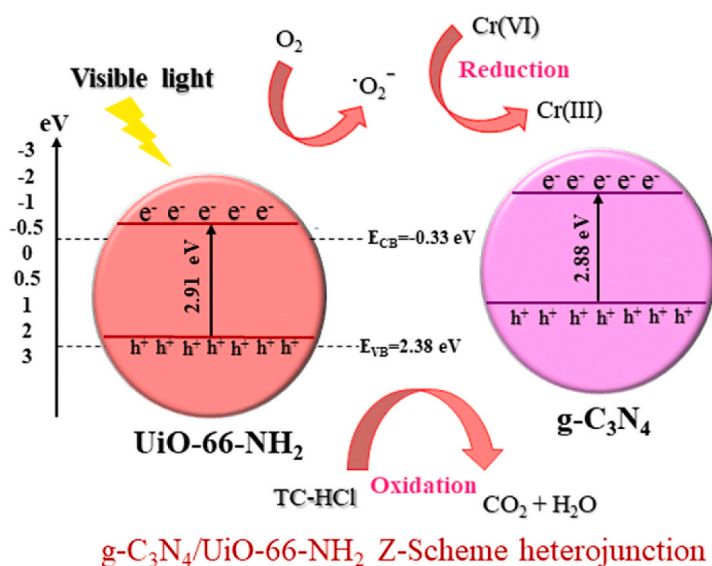


Fig. 9. Photocatalytic mechanism of CU for reduction of Cr(VI) and oxidation of TC-HCl [168].

Table 4
Degradation of various pollutants by MOFs Z-scheme heterojunctions.

Materials	Synthesis of method	Pollutants	Type of irradiation light	Time (min)	Degradation (%)	Ref.
PCN-222-PW ₂ /TiO ₂	Solvothermal	Rhodamine B	VIS	80	98.5	[174]
MOF-5/Ag ₃ PO ₄	In situ precipitation	Rhodamine B	VIS	40	98.5	[175]
CuWO ₄ /Bi ₂ S ₃ /ZIF-67 (Co)	Hydrothermal	Cephalexin	VIS	80	90	[176]
RP/MIL-101 (Fe)	Solvothermal	Tetracycline	Full spectrum	80	90	[177]
Co-MIL-53-NH ₂ -BT	Hydrothermal	Ofloxacin	VIS	120	100	[178]
g-C ₃ N ₄ /MIL-68 (In)-NH ₂	In situ solvothermal	Ibuprofen	VIS	180	93	[179]
Pt/MIL-125 (Ti)/Ag	Solvothermal	Ketoprofen	VIS	120	96	[180]
UiO-66 (Zr)/CdIn ₂ S ₄	Hydrothermal	Bisphenol A	UV	240	99.4	[181]
UiO-66(Zr)/ZnO/GO	Ultrasonic/Solvothermal	Malathion	VIS	90	100	[182]
Pt@UiO-66-NH ₂ (Zr) (PMR)	Hydrothermal	Phenol	Sun	300	70	[183]
NH ₂ -MIL-125 (Ti)	Solvothermal/	Dichlorophen and	VIS	210	98.6 and 97.5	[184]
@ZnIn ₂ S ₄ /CdS	Hydrothermal	Trichlorophenol				
g-C ₃ N ₄ /PDI@NH ₂ -MIL-53 (Fe)	Solvothermal	<i>p</i> -Nitrophenol	VIS	30	100	[185]
UiO-66-NH ₂ /Bi ₂ WO ₆	Ultrasonic/Solvothermal	Rhodamine B	VIS	90	100	[186]
MIL-53(Fe)/Bi ₁₂ O ₁₇ C ₁₂	Solvothermal	Cr(VI)	VIS	90	99.2	[187]
CuBi ₂ O ₄ /MIL-88A(Fe)	Hydrothermal	Cr(VI)	VIS	30	100	[188]
MIL-88A(Fe)/MoS ₂	Hydrothermal	Bisphenol-A	UV	60	98.2	[189]
SmVO ₄ /UiO-66-NH ₂	Hydrothermal	Tetracycline hydrochloride	Sun	90	50	[190]
MIL-101(Fe)/Bi ₂ WO ₆	Hydrothermal	Rhodamine B	VIS	15	96	[191]
Bi ₂ WO ₆ /Ni-MOF	Hydrothermal	Methylene blue	VIS	60	98.8	[192]
CuWO ₄ /Bi ₂ S ₃ /ZIF67	Hydrothermal	Metronidazole	VIS	80	95.6	[193]
CuWO ₄ /Bi ₂ S ₃ /ZIF67	Hydrothermal	Cephalexin	VIS	80	90.1	[193]
MIL-100(Fe)/α-Fe ₂ O ₃	Hydrothermal	O-xylene	VIS	200	100	[194]

through a straightforward approach involving mechanical grinding and low-temperature heating. The application of this synthesis technique led to the creation of composites that exhibit diverse light absorption abilities, long-term stability, and significant H₂ production through photocatalysis. In addition, these composites showed the optimal rate of H₂ production, which was 41, and 15 times higher than pure Zr-MOF, and g-C₃N₄, respectively. The increased charge separation and redox ability due to the heterogeneous charge transfer mechanism of Zr-MOF/g-C₃N₄ helped to increase the efficiency of H₂ production in photocatalysis. This discovery not only provides a rational approach to form heterogeneous junctions, but also provides a cost-effective alternative to MOF/g-C₃N₄ photocatalysts.

Koyale et al. [204] investigated the ability of Cu-based MOF sensitized ZnO nanorods (NRs) combined with multiwalled carbon nanotube (MWCNT) nanocomposites to split water through photoelectrochemical reactions, by synthesizing ZnO NRs, and ZnO NRs/MWCNTs nanocomposites with different MWCNT content and studying their structural, optical, and surface properties. Their results displayed that the incorporation of MWCNTs improved the optical and surface characteristics of the nanostructures, leading to enhanced photoelectrochemical performance. Their study provides valuable insights for the development of nanostructures and their composites for water splitting processes.

Liang et al. [205] have introduced a new method for synthesizing CeZnO/CdS NRs, which exhibited exceptional photocatalytic activity for H₂ production. The enhanced efficacy of these NRs can be ascribed to the establishment of a Z-scheme heterojunction, the incorporation of carbon, and the organized configuration of porous NRs, all of which efficiently diminished the rate at which electron-hole pairs recombine.

A successful creation of a novel Z-scheme CdLa₂S₄/MIL-88A(Fe) heterojunction has been achieved through the effective loading of CdLa₂S₄ onto MIL-88A(Fe) with a uniform anchoring, thus resulting in the formation of a highly efficient and promising semiconductor interface. The photocatalytic production of H₂ by the CdLa₂S₄/MIL-88A(Fe) composites exhibited remarkable efficiency, as evidenced by a maximum H₂-generation rate that is nearly 8 times higher than that of the pristine CdLa₂S₄ material. This significant enhancement in performance can be attributed to the presence of a distinctive Z-scheme structure within the composites, which plays an influential role in facilitating the efficient separation of electron-hole pairs [206].

Ding and colleagues [207] introduced a novel approach to fabricate photoelectrodes composed of ZnO/TiO₂, which are enriched with a significant number of oxygen vacancies. This was accomplished by effectively integrating ZIF-8 with TiO₂ NRs via the mechanism of electrostatic interaction. The resulting photoelectrodes showed enhanced electrical conductivity and charges separation, achieving a appreciably higher photocurrent density and incident photon-to-electron conversion efficiency compared to pure TiO₂.

In their study, Li et al. [200] undertook an examination of g-C₃N₄, a highly regarded photocatalyst with great potential. They investigated the properties and applications of g-C₃N₄, particularly in the realm of photocatalytic water splitting for the evolution of H₂. This process, however, typically relies on the use of noble metal co-catalysts, thereby leading to elevated costs associated with its implementation. In their investigation, a hybrid material comprising Co@N doped-carbon/g-C₃N₄ was synthesized by subjecting ZIF-67 and melamine to a thermal condensation process. The resultant Co@N doped-carbon/g-C₃N₄ composites exhibited remarkable catalytic activity in the H₂ evolution during the water splitting process, avoiding the requirement for any noble metal co-catalysts, even when exposed to simulated sunlight. This noteworthy finding underscores the potential of the Co@N doped-carbon/g-C₃N₄ composite

as a promising alternative for efficient solar-driven H₂ evolution. Due to the effective absorption of electrons by Co@N doped-carbon/g-C₃N₄/ZIF-67, the H₂ production rate is 6 times higher than that of pure g-C₃N₄. Further information about water splitting by Z-scheme heterojunction MOFs can be found in Table 5.

According to studies found in the literature, Z-scheme heterojunction MOFs photocatalysts utilizing zirconium exhibit superior performance in the process of water splitting, mainly attributed to their exceptionally large surface area and robust stability.

5. Density functional theory calculations and degradation pathways

Dong et al. [208] have effectively produced a new composite consisting of AgI/MOF-808 by in situ precipitation hydrothermal method. This groundbreaking synthesis technique uses high temperature and pressure to create composite materials. Using XPS and density functional theory (DFT) methods, the research team validated the direction of electron migration inside the composite. These analyses provided conclusive evidence for the existence of a single-photon excitation pathway, which is crucial for the photocatalytic properties of the composite. Note that the AgI/MOF-808 composite demonstrates an adsorption capacity of 1890.01 mg/g, which shows its exceptional ability to adsorb pollutants. This is an important finding because it exhibits the potential of composites in wastewater and environmental treatment. In addition, this composite showed significant photocatalytic activity towards TC-HCl, a pollutant commonly found in water sources. This means that the synthesized composite can effectively degrade TC-HCl, which is a promising result to address the issue of water pollution. This research team utilized electrochemical and PL methods to further investigate the optical properties of the composite. These experiments revealed that AgI components within the composite, which accounted for 40% of the total weight, showed the highest photocarrier transport efficiency and separation efficiency. This discovery is significant because it emphasizes the impact of AgI on improving the performance of composites, leading to an impressive 83.02% degradation efficiency of TC-HCl and a degradation rate approximately 14 times higher than pure AgI. DFT calculations and ultra-high-performance liquid chromatography-MS/MS (UHPLC-MS/MS) were used to identify intermediate degradation products and investigate potential degradation pathways using condensed Fukui function (CFF), highest occupied molecular orbital (HOMO), and least unoccupied molecular orbital (LUMO) to predict reaction sites. A 3D Fukui function diagram was constructed to show nucleophilic, electrophilic, and free radical attacks. The vulnerability of TCH regions to electron deprivation was demonstrated by electrostatic potential (ESP) plotting, while Frontier molecular orbital analysis failed to accurately predict the attack type. The CFF value and level map were determined using Hirshfeld's load, and higher values indicated more attack sensitivity. Consequences of nucleophilic, electrophilic, and free radical attack considerably influence the degradation pathway of TC-HCl. This effect is primarily driven by the activating species $\cdot\text{O}_2^-$ and $\cdot\text{OH}$, which act as primary activators, while the secondary activator H^+ also plays an important role. The effects of these types of activators and agents on the path of TC-HCl degradation are of considerable importance and cannot be ignored (Fig. 10). The synthesized AgI/MoF-808 composite has shown great promise in wastewater treatment and environmental treatment. Its exceptional adsorption capacity, remarkable photocatalytic properties, and high degradation efficiency make it an ideal candidate for addressing the urgent water pollution problem. The findings presented in this study provide valuable insight into the potential applications of composites and open new possibilities for future research in this field [208].

A self-cleaning membrane reactor, PENS/TA/ZIF-67 @Ag₂S (PZA), was developed using the non-solvent-induced phase separation (NIPS) method, which showed high efficiency and flux in oil-water emulsion experiments [209]. This reactor also exhibited a high sulfamethoxazole (SMX) degradation rate and suggested a practical approach to developing efficient and environmentally friendly antibiotic polymer membrane reactors. DFT calculations were used to investigate and analyze the degradation mechanisms of SMX. The main goal of their research was to evaluate the electron gain or loss capacities of the HOMO and the LUMO. After conducting the analysis, it was found that the oxazole, sulfonamide, and benzene ring groups are the primary locations of the HOMO of SMX, making them highly susceptible to electrophilic radical attacks. In contrast, the cyclic groups of benzene and sulfonamide contain the main location of the LUMO, resulting in the creation of reactive intermediates. By understanding the specific locations of these molecular orbitals and their associated vulnerability to attack, we can gain valuable insight into the degradation mechanism of SMX (Fig. 11) [209].

The implementation of heterojunction interfaces has demonstrated itself to be a highly successful approach in attaining optimal charge separation and improving the performance of photocatalysis [210]. This is demonstrated by evaluating the photocatalytic efficiency of Bi₂WO₆/Bi-MOF heterojunction. As a result of this evaluation, an optimized Bi₂WO₆/Bi-MOF photocatalyst has been identified with impressive degradation efficiency, reaching a remarkable 96% for RhB and 80% for TC-HCl in 60 min. The assessment

Table 5
Water splitting by MOFs Z-scheme heterojunctions.

Photocatalysis	H ₂ evolution rate	Ref.
ZnCo ₂ S ₄ /MOF-199	11.6 mmol g ⁻¹ h ⁻¹	[195]
MgIn ₂ S ₄ /UiO-66- NH ₂	493.8 μmol h ⁻¹	[196]
Zr-MOF/g-C ₃ N ₄	1.252 mmol h ⁻¹ g ⁻¹	[197]
HPW/Zr ₆ O ₄ (OH) ₄ (BDC) ₆ (UiO-66)	353.89 μmol h ⁻¹	[198]
α-SnWO ₄ /UiO-66(NH ₂)/g-C ₃ N ₄	105 μmol g ⁻¹ h ⁻¹	[199]
(ZIF-67) derived Co@NC/g-C ₃ N ₄	5098.12 μmol g ⁻¹ h ⁻¹	[200]
NiS-PCN	1239.3 μmol g ⁻¹ h ⁻¹	[201]
CdS/NH ₂ -MIL-125(Ti)	6.62 mmol g ⁻¹ h ⁻¹	[202]
ZIF-67/Co ₃ O ₄	2.016 mmol g ⁻¹ h ⁻¹	[203]

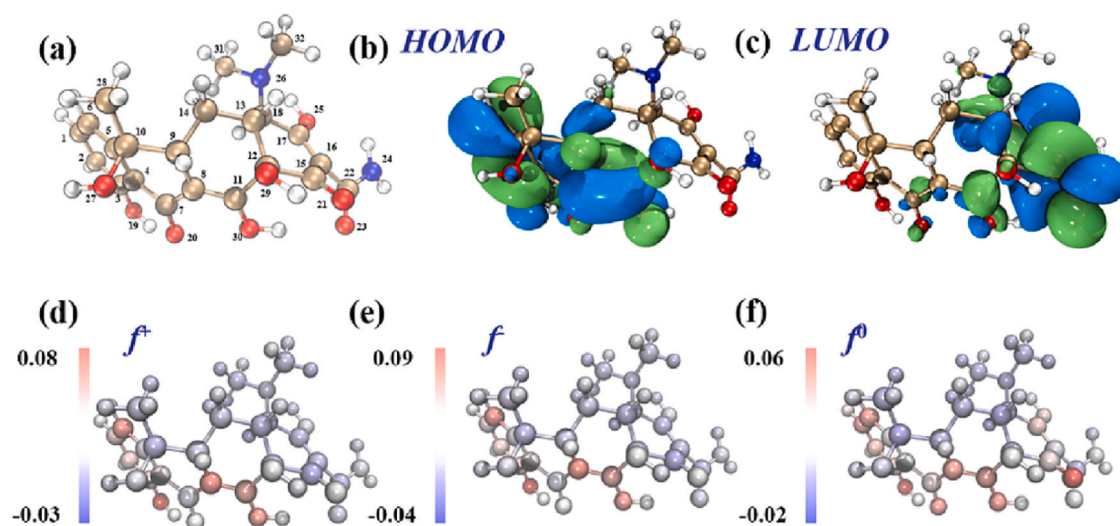


Fig. 10. a) Optimized TC-HCl structure, b) HOMO orbitals of TC-HCl, c) LUMO orbitals of TC-HCl, d) nucleophilic attack, e) electrophilic attack, and f) radical attack electrostatic potential diagram of TCH, white (hydrogen), blue (nitrogen), gold (carbon), and red, (oxygen). Reproduced from Ref. [208] with a Copyright permission 2023, Elsevier B.V.

was reinforced by a systematic DFT analysis of the BSs and density of states of the materials, providing insights into the underlying mechanisms driving the improved photocatalytic activity [211]. The findings have shown interesting insights into the electronic properties of Bi-MOF and Bi_2WO_6 materials. In particular, it was observed that Bi-MOF has a direct BG, while Bi_2WO_6 has an indirect BG, which is consistent with previous conclusions. Further investigation of the density of states has discovered the combination of the maximum CB and the lowest CB of both materials. The VB maximum in Bi-MOF consists mainly of Bi6s, O2p, and C2s orbitals, while the CB minimum primarily comprises Bi6p orbitals. In contrast, for Bi_2WO_6 , the VB maximum and CB minimum include the Bi6s and O2p orbitals as well as the Bi6p and W4d orbitals, resulting in BG values of approximately 2.59 eV for Bi-MOF and 1.88 eV for Bi_2WO_6 (Fig. 12) [211].

Zhao et al. [212] developed a heterojunction photocatalyst called $\text{Bi}_5\text{O}_7\text{i}/\text{UiO}-66\text{-NH}_2$ (BU) with a direct Z-scheme to improve the degradation of ciprofloxacin (CIP). They have focused on gaining insight into the mechanism, performing pathway analysis, and evaluating the toxicity associated with this innovative approach. The ball milling technique was used to synthesize direct photocatalysts of Z-scheme BU. Then, their photocatalytic activity was evaluated using CIP as a model compound of particular interest to investigate the heterojunction content of $\text{UiO}-66\text{-NH}_2$, especially the 50% w/w composition (BU-5), which showed exceptional structural stability. Impressively, under the influence of 120 min of illumination, the BU-5 material achieved a remarkable 96.1% efficiency in CIP removal, as shown by accompanying photographic evidence. By examining the complexities of the degradation process, it was observed that the formation of cavities plays an important role in addition to the involvement of $\cdot\text{O}_2^-$ and h^+ . Zhao et al. [212] highlighted the importance of their findings, which elucidated the unique configuration of charge transport exhibited by oxyhalide-based heterojunction photocatalysts and bismuth-rich MOFs. On the other hand, this arrangement of components provides remarkable abilities to transfer electrons between molecules and therefore presents a hopeful resolution for eliminating antibiotics. Upon closer inspection, they also noted the deposition of Pt NPs, mainly in the vicinity of the octagonal $\text{UiO}-66\text{-NH}_2$. The observations reinforced the concept that BU-5 adheres to the charge transfer process along with a Z-scheme. The charge transfer mechanism between $\text{UiO}-66\text{-NH}_2$ and $\text{Bi}_5\text{O}_7\text{i}$ has been confirmed by Bader charge simulation calculations, thus validating the above concept. These calculations demonstrated that electrons migrate from $\text{Bi}_5\text{O}_7\text{i}$ to $\text{UiO}-66\text{-NH}_2$. It is worth noting that Fig. 13 presents two important components. A high-resolution transmission electron microscopy (HRTEM) image showed the presence of Pt NPs deposited on the BU-5 material (Fig. 13(a)). A complex structure model of the $\text{Bi}_5\text{O}_7\text{i}/\text{UiO}-66\text{-NH}_2$ heterojunction bond is shown, in which different atom colors are used to represent distinct entities (Fig. 13(b)). The comprehensive insight gained from this particular study serves as a valuable foundation for future developments in photocatalysis and antibiotic removal [212].

Yang and his colleagues [212] conducted a study on the degradation of TC through photocatalysis by employing Ag_3PO_4 /mixed-valence MIL-88A(Fe) (AMM) heterojunctions within a Z-scheme system. This research group intended to explore the depth of knowledge regarding the complex functioning of the mechanism, the pathways through which degradation occurs, and the accurate calculation of the corresponding DFT, an essential tool in computational chemistry. Z-scheme heterojunctions of AMM were constructed using an in-situ generated photo-fenton process, resulting in optimized AMM-20 heterojunctions with superior photocatalytic activity compared to pristine Ag_3PO_4 and MIL-88A(Fe) [213]. The Z-scheme transport pathway improved photocatalytic corrosion inhibition and light stability by increasing the charge carrier transfer rate. However, adjusting the FeI/FeIII MIL-88A (Fe) ratio with mixed capacitance further enhanced these effects. The photo-fenton process increased the photocatalytic efficiency by producing in situ, as verified by experiments such as free radical trapping measurements, in situ XPS and ESR measurements, fluorescence analysis,

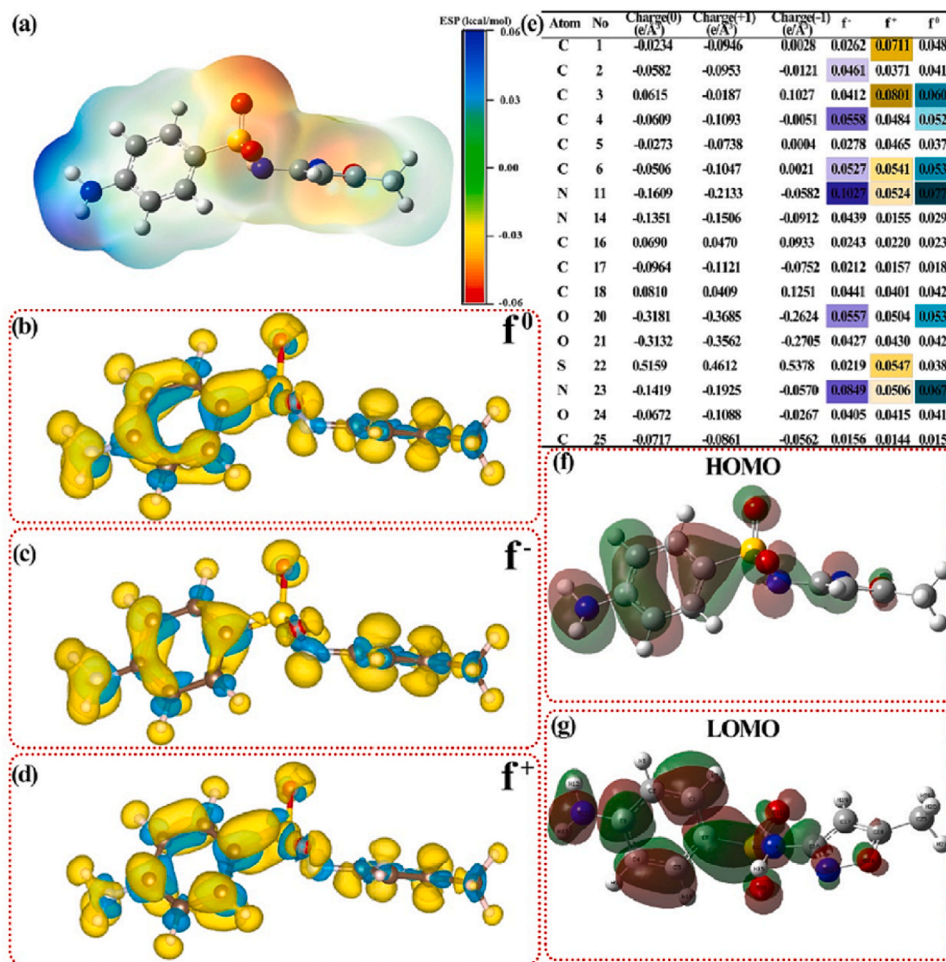


Fig. 11. The SMX molecules calculated by DFT: a) ESP-mapped molecular surface of SMX, b) radical, c) electrophilic, d) nucleophilic values, e) NPA and Fukui index of SMX, f) HOMO, and g) LUMO. Reproduced from Ref. [209] with a Copyright permission 2023, Elsevier B.V.

and degradation pathways. The researchers investigated the possibility of enhancing the photocatalytic efficiency of MIL-88A (Fe) by manipulating the FeI/FeIII ratio. This particular research avenue was substantiated by findings obtained through computational analysis, which in turn illuminates a promising approach to increase the effectiveness of photocatalytic materials through simple chemical modifications [213]. The BS results for the samples are displayed in Fig. 14.

Zhang et al. [214], achieved successful synthesis of the Cu_{0.5}Co_{0.5}-ZIF@Fe₂O₃@CC-150 heterojunction, named Cu_{1-x}Co_x-ZFC-150, which displayed outstanding performance in hydrogen evolution reaction (HER), and oxygen evolution reaction (OER) reactions with low overpotential and a small Tafel slope. The Cu_{1-x}Co_x-ZFC-150, acting as both an anode and cathode, achieved a cell voltage of 1.62 V and demonstrated high efficiency in converting CO₂ into CO and CH₄ through photocatalysis; the reasons for its improved OER kinetics and photocatalytic properties were examined in detail using experimental observations and DFT analysis within the framework of the Z-scheme charge transfer model.

Using ZIF-67 as a precursor, Han et al. [203], accomplished the synthesis of Co₃O₄ NPs that were enriched with oxygen vacancies. By anchoring nanoparticles on a polyamide (PI) surface, a Z-scheme hybrid heterojunction was fabricated. The resultant interfacial architecture between the Co₃O₄ NPs and PI demonstrated a robust interfacial electronic interaction, thereby extending the range of light absorption in the VIS spectrum and increasing the rate of charge transfer. DFT calculations have confirmed the Z scheme in this hybrid bond and have shown that the electron transfers from CB Co₃O₄ to VB PI hindered the electron transfer between Co₃O₄ and PI, leading to reduced electron-hole recombination in PI and increased hydrogen production.

The disintegration process of diverse contaminants was examined through DFT computations and it has been validated that photocatalysts founded on Z-scheme heterojunction MOFs exhibit considerable promise for pragmatic utilization in the elimination of emerging contaminants from water treatment systems.

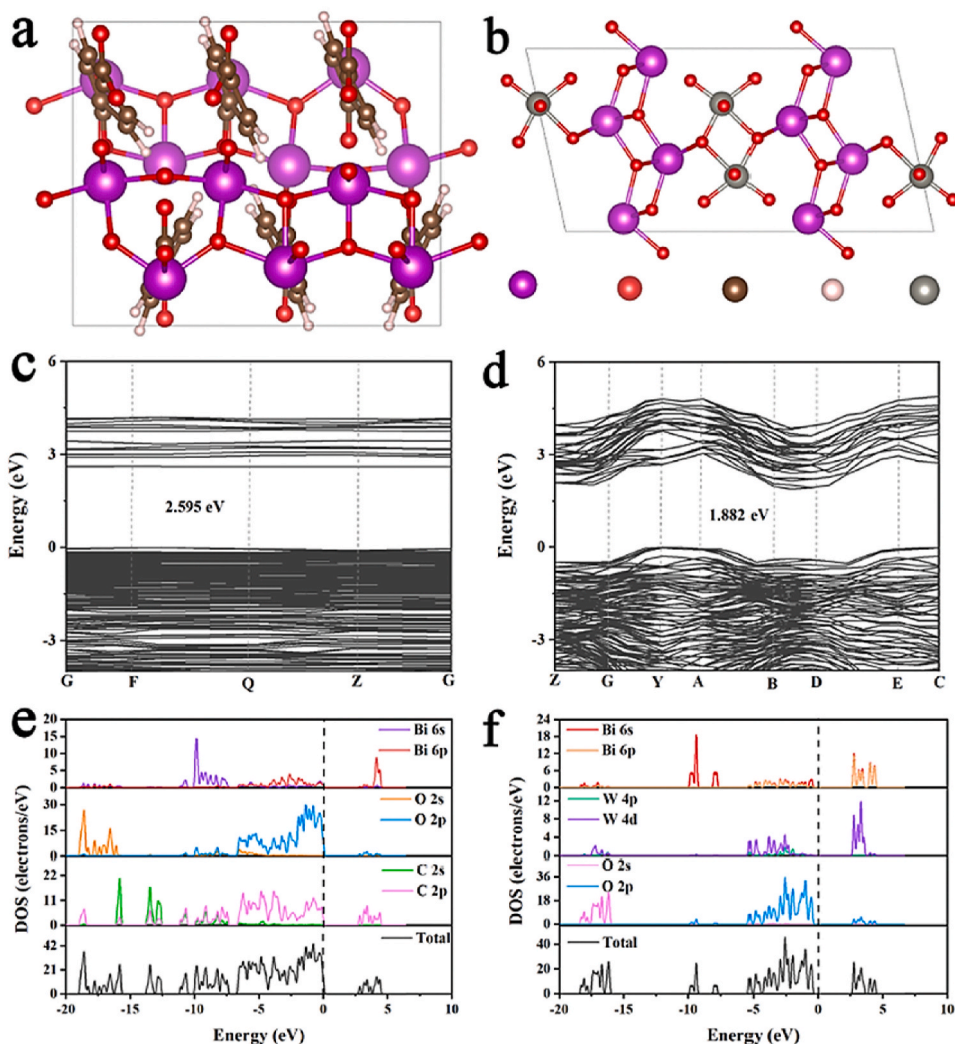


Fig. 12. Crystal structure of a) Bi-MOF, and b) Bi₂WO₆; BSs of c) Bi-MOF, and d) Bi₂WO₆; and density of states of e) Bi-MOF, and f) Bi₂WO₆. Reproduced from Ref. [211], with permission from the Copy right 2023, Elsevier B.V.

6. Challenges and future directions

The extensive and comprehensive research on MOFs Z-scheme heterojunctions demonstrates the wide range of potential applications that these materials have. It should be emphasized and acknowledged that despite the numerous multifunctional advantages resulting from Z-Scheme microporous MOFs, there are still challenges that need to be carefully investigated and resolved.

Approximately half of the electrons produced within the MOFs Z-scheme heterojunctions structure undergo a process known as recombination, which introduces uncertainty regarding the superiority of Z-scheme architectures in facilitating charge separation when compared to conventional type II architectures and the verification of the load-carrying path using the solid-state MOFs Z-scheme still remains uncertain. The MOFs Z-scheme charge transfer is anticipated to transpire between the n-type semiconductor and the p-type semiconductor, with both types of photocatalyst particles operating as miniature photoanodes and photocathodes. Additionally, for the electron transfer in the MOFs Z-scheme to be sufficiently driven, there should be an overlap in the photoinduced/cathode over potential of both n- and p-types. From a thermodynamic standpoint, it is improbable for solid-state MOFs Z-scheme heterostructures to form between two n-type semiconductors or two p-type semiconductors, despite certain empirical claims made by different sources.

Commercialization and validation of the MOFs Z-scheme pose a major challenge, primarily because it requires high collaboration between academic institutions and industry. However, despite the additional hurdles that may arise in an industrial setting, there is a prevailing optimism that these materials can be effectively produced on a pilot scale. However, comprehensive exploration and further research on Z-scheme heterojunction MOFs have the potential to enhance their properties. To achieve the desired result, various factors such as availability and cost of raw materials, conditions and method of synthesis, optimal mechanism, high performance, low

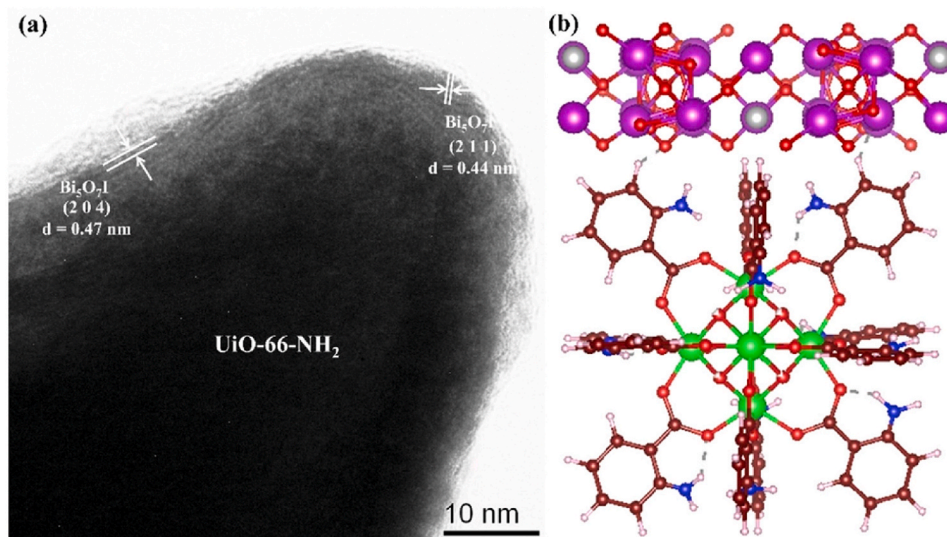


Fig. 13. a) An HRTEM image of Pt NPs photo-deposited over BU-5 and b) the BU-5 heterojunction with optimal structure model, represented by various atom colors. Reproduced from Ref. [212] with a Copyright permission 2021, Elsevier B.V.

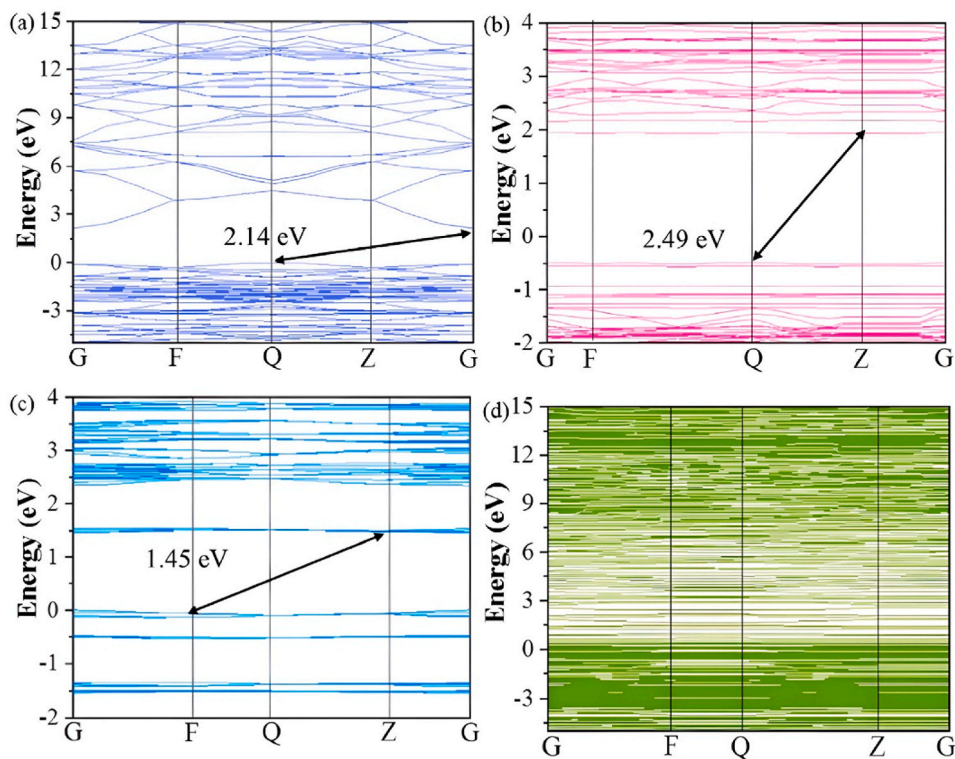


Fig. 14. BS of a) Ag_3PO_4 , b) MIL-88A(Fe), c) m-MIL-88A(Fe), and d) AMM heterojunction. Reproduced from Ref. [213] with a Copyright permission 2021, Elsevier B.V.

impurity, and minimal solvent consumption should be considered. In addition, one of the key parameters of MOFs Z-scheme heterojunction is their regeneration process after saturation to reuse them in successive cycles. Therefore, disposal, regeneration, and recycling methods of MOFs Z-scheme heterojunctions are important at industrial scales, especially in terms of energy saving and competitive operating costs. Regeneration conditions depend on the choice of solvents, temperature, pressure, kinetics of desorption, and the stability of MOFs Z-scheme heterojunctions. Efforts should focus on developing new techniques for the regeneration of MOFs to

overcome the obstacles associated with their regeneration effectively. These challenges include degradation in the design of MOFs Z-scheme during disposal and application of these materials on an industrial scale. It is necessary to maintain the heterogeneous structure and porosity of MOFs Z-scheme during the regeneration process. Therefore, the focus should be on exploring innovative methods to overcome these obstacles and maintain the integrity of MOFs Z-scheme. Owing to the recent advancements in research about the MOFs Z-scheme heterojunction, it is anticipated that significant headway will be made in developing MOFs' Z-scheme heterojunctions to further their characteristics and applications. It is believed that additional refinement of the synthesis process for Z-scheme heterojunction photocatalysts based on MOFs and the investigation of their photocatalytic efficiency will greatly enhance the implementation of heterojunction photocatalytic materials. This, in turn, will aid in advancing the goal of creating an environmentally friendly planet and fostering the sustainable progress of human civilization.

6.1. Summary and conclusions

In recent years, advanced materials with desirable properties have been increasingly used as a unique strategy to reduce the harmful effects of environmental pollution, especially in water and wastewater domains. The noteworthy performance capabilities of MOFs Z-scheme heterojunction with porous network and high selectivity hold paramount significance in wastewater treatment. Specifically, MOFs Z-scheme heterojunction nanostructured composites exhibit immense potential for deployment in cleanup and environmental monitoring because of their unparalleled preparation and performance. MOFs Z-scheme heterojunction photocatalysts have a remarkable potential to facilitate oxidation reactions, thereby enabling highly efficient degradation of organic compounds through photocatalytic processes. In addition, these photocatalysts with high capacity appear to be effective in reduction reactions; this will further increase their overall performance in terms of photocatalytic degradation. Therefore, the use of Z-scheme MOFs photocatalysts in environmental processes is promising. Investigating the performance of MOFs Z-scheme heterojunction photocatalysts has revealed that nucleophilic, electrophilic, and free radical attack mechanisms have significant effects on the overall efficiency of the pollutant degradation processes. Additionally, it is necessary to adopt environmentally conscious and economical methodologies, thus ensuring their practicality and the possibility of real scenarios to implement these nanostructures in wastewater treatment and management. Researchers should consider efficient preparation techniques and cost optimization as key aspects to save resources and simplify processes. At the same time, they should discover effective ways to increase selectivity and reusability. Consequently, future research should focus on enhancing the design capabilities of MOFs Z-scheme heterojunction for practical applications. In this context, future research efforts should focus on implementing new, efficient, and practical methods on industrial scales. Among the various synthesis approaches for Z-scheme heterojunction MOFs, hydrothermal and solvothermal techniques stand out as the predominant methods due to their exceptional performance, making them ideal for large-scale industrial applications. To achieve this goal, it is important to strictly follow the recommended measures to lay the groundwork for the successful industrial application of environmentally friendly MOFs Z-scheme. It is necessary to choose the heterogeneity of MOFs Z-scheme as a material resistant to structural degradation caused by various factors such as moisture, acid, base, and radiation.

H₂, being a significant energy carrier compared to other fuels, possesses the capability to be transformed into alternative forms of energy with remarkable efficiency and environmentally friendly combustion. Presently, the utilization of photocatalytic production of H₂ using MOF compounds holds particular significance due to environmental concerns and the need for accessing renewable energies. This process involves the production of H₂ from abundant and renewable natural sources such as water and solar energy, which have a more secure impact on the environment in comparison to fossil fuels. Within the photocatalytic H₂ production process by MOF, the energy level of the BG of the structure, crystal defects, and the morphology of the photocatalyst particles play a crucial role. The pH, photocatalyst concentration, and the solution's turbidity also influence the process of photocatalytic H₂ production. To address the drawbacks of MOFs and enhance their effectiveness in the process of H₂ production from water splitting, various materials and methods are employed such as the modification of the MOF particle surface with metal ions, and carbon dots. These modifications enhance the photocatalytic properties of MOFs, resulting in improved light absorption within the VIS region.

By employing a heterojunction model, MOFs Z-scheme demonstrate a high level of efficiency in the photocatalytic water splitting in the presence of sunlight. Indeed, MOFs Z-scheme introduce a novel, cost-effective approach to the photocatalytic water splitting using solar energy. Studies indicate that Z-scheme heterojunction MOFs with zirconium show high efficiency in water splitting due to their large surface area and stability. To successfully commercialize the process of H₂ production through photocatalytic water splitting, it becomes imperative to utilize inexpensive materials that are resistant to photocorrosion, thus enabling the potential for energy and cost recovery from the initial investment. While MOFs Z-scheme have the potential to serve as suitable photocatalysts in this field, the associated drawbacks necessitate further research and investigation in order to overcome them and achieve the commercialization of this process. Thus, future research should use the heterogeneity of MOFs Z-scheme by overcoming the existing challenges.

ABBREVIATIONS

2D, Two-dimensional	MO, Methyl orange
3D, Three-dimensional	MOFs, Metal-organic frameworks
AOPs, Advanced oxidation processes	MWCNTs, Multiwalled carbon nanotube
BET, Brunauer-Emmett-Teller	NPs, Nanaoparticles
BG, Band gap	NRs, Nanorods
BJH, Barrett-Joyner-Halenda	NIPS, Nonsolvent-induced phase separation
BOD, Biochemical oxygen demand	OER, Oxygen evolution reaction

(continued on next page)

(continued)

BS, Band structure,	OFL, Ofloxacin
CB, Conduction band	O ₂ , Oxygen
CFF, Condensed Fukui function	PI, Polyimide
COD, Chemical oxygen demand	PS I, Photosystem I
COFs, Covalent organic frameworks	PS II, Photosystem II
CTO-CN, CoTiO ₃ /g-C ₃ N ₄	PL, Photoluminescence
DFT, Density functional theory	PZA, PENS/TA/ZIF-67@Ag ₂ S
DRS, Diffuse reflectance spectroscopy	QDs, Quantum dots
EPR, Electron paramagnetic resonance	RhB, Rhodamine B
E _{VB} , Edge of the valence band	ROS, Reactive oxygen species
FESEM, Field emission scanning electron microscopy	SC, Sodium alginate-kappa-carrageenan
FTIR, Fourier transform infrared spectroscopy	SMX, Sulfamethoxazole
GC-MS, Gas chromatography-mass spectroscopy g-C ₃ N ₄ , Graphitic carbon nitride	TC-HCl, Tetracycline hydrochloride
HER, Hydrogen evolution reaction	TEST, Toxicity Estimation Software Tool
HRTEM, High-resolution transmission electron microscopy	TTA, 4,4',4''-(1,3,5-triazine-2,4,6-triyl)trianiline
HOMO, Highest occupied molecular orbital	TTB, 4,4',4''-(1,3,5-triazine-2,4,6-triyl)tribenzaldehyde
H ₂ , Hydrogen	UHPLC-MS/MS, Ultra-high performance liquid chromatography-MS/MS
LDH, Layered double hydroxides	UIO, University of Oslo
LMCT/MLCT, Ligand-to-metal/metal-to-ligand charge transfer	VB, Valence band
LUMO, Least unoccupied molecular orbital	VIS, Visible VIS
MB, Methylene Blue	XPS, X-ray photoelectron spectroscopy
MCN, Modified g-C ₃ N ₄	XRD, X-ray diffraction
	ZIF, Zeolitic Imidazolate Frameworks

Data availability statement

All relevant data and material are presented in the paper. Also, this review paper has not generated new data.

Consent for publication

Not applicable.

Ethics approval and consent to participate

Not applicable.

CRedit authorship contribution statement

Narges Elmi Fard: Investigation, Formal analysis, Data curation, Writing – original draft. **Nisreen S. Ali:** Conceptualization, Investigation, Writing – review & editing. **Noori M. Cata Saady:** Data curation, Conceptualization, Formal analysis, Writing – review & editing. **Talib M. Albayati:** Methodology, Investigation, Data curation, Conceptualization. **Issam K. Salih:** Formal analysis, Methodology. **Sohrab Zendeheboudi:** Investigation, Conceptualization, Formal analysis, Writing – review & editing. **Hamed N. Harharah:** Investigation, Writing – review & editing. **Ramzi H. Harharah:** Methodology, Writing – review & editing.

Declaration of competing interest

The authors declare that they have no known competing financial interests or personal relationships that could have appeared to influence the work reported in this paper.

Acknowledgments

The authors are grateful to the Department of Chemistry, Science and Research Branch, Islamic Azad University, Tehran, Iran; the Departments of Civil Engineering & Process Engineering, Memorial University, St. John's, NL, Canada; the Materials Engineering Department, College of Engineering, Mustansiriyah University, Baghdad, Iraq; the Department of Chemical Engineering, the University of Technology-Iraq, Baghdad, Iraq; and the Department of Chemical and Petroleum Industries Engineering, Al-Mustaqbal University, Babylon, Iraq.

References

- [1] A. Mukhopadhyay, S. Duttagupta, A. Mukherjee, Emerging organic contaminants in global community drinking water sources and supply: a review of occurrence, processes and remediation, *J. Environ. Chem. Eng.* 10 (3) (2022) 107560.
- [2] C. Yan, J. Jin, J. Wang, F. Zhang, Y. Tian, C. Liu, Q. Han, Metal-organic frameworks (MOFs) for the efficient removal of contaminants from water: underlying mechanisms, recent advances, challenges, and future prospects, *Coord. Chem. Rev.* 468 (2022) 214595.

- [3] S. Rasouli, N. Rezaei, H. Hamed, S. Zendejboudi, X. Duan, Superhydrophobic and superoleophilic membranes for oil-water separation application: a comprehensive review, *Mater. Des.* 204 (2021) 109599.
- [4] N. Elmi Fard, R. Fazaeli, Fabrication of superhydrophobic CoFe_2O_4 /polyaniline/covalent organic frameworks/cotton fabric membrane and evaluation of its efficiency in separation of olive oil from water, *J. Chin. Chem. Soc.* 69 (12) (2022) 2014–2026.
- [5] M. Maheri, C. Bazan, S. Zendejboudi, H. Usefi, Machine learning to assess CO_2 adsorption by biomass waste, *J. CO₂ Util.* 76 (2023) 102590.
- [6] S. Zhao, J. Jiang, C. Zhang, F. Chen, Y. Song, Y. Tang, Construction of a novel double S-scheme heterojunction $\text{CeO}_2/\text{g-C}_3\text{N}_4/\text{Bi}_2\text{O}_3$ for significantly boosted degradation of tetracycline: insight into the dual charge transfer mode, *Chem. Eng. J.* 479 (2024) 147333.
- [7] F. Meng, Z. Fan, C. Zhang, Y. Hu, T. Guan, A. Li, Morphology-controlled synthesis of CeO_2 microstructures and their room temperature ferromagnetism, *J. Mater. Sci. Technol.* 33 (5) (2017) 444–451.
- [8] L. Wang, F. Meng, K. Li, F. Lu, Characterization and optical properties of pole-like nano- CeO_2 synthesized by a facile hydrothermal method, *Appl. Surf. Sci.* 286 (2013) 269–274.
- [9] F. Meng, L. Wang, J. Cui, Controllable synthesis and optical properties of nano- CeO_2 via a facile hydrothermal route, *J. Alloys Compd.* 556 (2013) 102–108.
- [10] L. Wang, F. Meng, Oxygen vacancy and Ce^{3+} ion dependent magnetism of monocrystal CeO_2 nanopoles synthesized by a facile hydrothermal method, *Mater. Res. Bull.* 48 (9) (2013) 3492–3498.
- [11] Z. Fan, F. Meng, J. Gong, H. Li, Y. Hu, D. Liu, Enhanced photocatalytic activity of hierarchical flower-like $\text{CeO}_2/\text{TiO}_2$ heterostructures, *Mater. Lett.* 175 (2016) 36–39.
- [12] Z. Fan, F. Meng, M. Zhang, Z. Wu, Z. Sun, A. Li, Solvothermal synthesis of hierarchical TiO_2 nanostructures with tunable morphology and enhanced photocatalytic activity, *Appl. Surf. Sci.* 360 (2016) 298–305.
- [13] F. Meng, Z. Sun, A mechanism for enhanced hydrophilicity of silver nanoparticles modified TiO_2 thin films deposited by RF magnetron sputtering, *Appl. Surf. Sci.* 255 (13–14) (2009) 6715–6720.
- [14] S. Abdolmohammadi, S.R. Nasrabadi, A. Seif, N.E. Fard, Ag/CdS nanocomposite: an efficient recyclable catalyst for the synthesis of novel 8-aryl-8H-[1, 3] dioxolo [4, 5-g] chromene-6-carboxylic acids under mild reaction conditions, *Comb. Chem. High Throughput Screen.* 21 (5) (2018) 323–328.
- [15] N.E. Fard, I. Raieisi, Z. Yousefpour, R. Mosavin, Review of metal sulfide-based MXene nanocomposites for environmental applications, gas sensing, energy storage, and photothermal therapy, *ACS Appl. Nano Mater.* 7 (6) (2024) 5698–5728.
- [16] Y. Liu, X. Xu, Z. Shao, Metal-organic frameworks derived porous carbon, metal oxides and metal sulfides-based compounds for supercapacitors application, *Energy Storage Mater.* 26 (2020) 1–22.
- [17] M. Safaei, M.M. Foroughi, N. Ebrahimipour, S. Jahani, A. Omid, M. Khatami, A review on metal-organic frameworks: synthesis and applications, *TrAC, Trends Anal. Chem.* 118 (2019) 401–425.
- [18] K. Poonia, S. Patial, P. Raizada, T. Ahamad, A.A.P. Khan, Q. Van Le, P. Singh, Recent advances in Metal Organic Framework (MOF)-based hierarchical composites for water treatment by adsorptive photocatalysis: a review, *Environ. Res.* (2023) 115349.
- [19] R. Seetharaj, P.V. Vandana, P. Arya, S. Mathew, Dependence of solvents, pH, molar ratio and temperature in tuning metal organic framework architecture, *Arab. J. Chem.* 12 (3) (2019) 295–315.
- [20] C.C. Wang, X. Wang, W. Liu, The synthesis strategies and photocatalytic performances of TiO_2 /MOFs composites: a state-of-the-art review, *Chem. Eng. J.* 391 (2020) 123601.
- [21] C.C. Wang, X. Ren, P. Wang, C. Chang, The state of the art review on photocatalytic Cr (VI) reduction over MOFs-based photocatalysts: from batch experiment to continuous operation, *Chemosphere* 303 (2022) 134949.
- [22] B. Shao, Z. Liu, G. Zeng, Y. Liu, X. Yang, C. Zhou, M. Yan, Immobilization of laccase on hollow mesoporous carbon nanospheres: noteworthy immobilization, excellent stability and efficacious for antibiotic contaminants removal, *J. Hazard Mater.* 362 (2019) 318–326.
- [23] G. Maurin, C. Serre, A. Cooper, F. Férey, The new age of MOFs and of their porous-related solids, *Chem. Soc. Rev.* 46 (11) (2017) 3104–3107.
- [24] Y. Liu, Z. Liu, D. Huang, M. Cheng, G. Zeng, C. Lai, B. Shao, Metal or metal-containing nanoparticle@ MOF nanocomposites as a promising type of photocatalyst, *Coord. Chem. Rev.* 388 (2019) 63–78.
- [25] L. Song, X. Jin, A. Zada, D. Hu, Z. Li, R. Yan, L. Jing, Modifying MOF-derived hollow BiVO_4 architecture with copper tetraphenylporphyrin as high-efficiency wide-visible-light Z-scheme heterojunction photocatalyst for 2-chlorophenol degradation, *J. Environ. Chem. Eng.* 11 (3) (2023) 110069.
- [26] B. Yu, Y. Wu, F. Meng, Q. Wang, X. Jia, M.W. Khan, H. Wu, Formation of hierarchical $\text{Bi}_2\text{MoO}_6/\text{In}_2\text{S}_3$ S-scheme heterojunction with rich oxygen vacancies for boosting photocatalytic CO_2 reduction, *Chem. Eng. J.* 429 (2022) 132456.
- [27] H. Wei, F. Meng, H. Zhang, W. Yu, J. Li, S. Yao, Novel oxygen vacancy-enriched $\text{Bi}_2\text{MoO}_6\text{-x}/\text{MoS}_2$ S-scheme heterojunction for strengthening photocatalytic reduction CO_2 and efficient degradation of levofloxacin hydrochloride: mechanism, DFT calculations, *J. Mater. Sci. Technol.* 185 (2024) 107–120.
- [28] Y. Yuan, R.T. Guo, L.F. Hong, X.Y. Ji, Z.D. Lin, Z.S. Li, W.G. Pan, A review of metal oxide-based Z-scheme heterojunction photocatalysts: actualities and developments, *Mater. Today Energy* 21 (2021) 100829.
- [29] W.A. El-Yazeed, A.I. Ahmed, Photocatalytic activity of mesoporous WO_3/TiO_2 nanocomposites for the photodegradation of methylene blue, *Inorg. Chem. Commun.* 105 (2019) 102–111.
- [30] K. Zheng, H. Liu, C. Nie, X. Zhang, H. Hu, G. Ma, J. Huo, Controllable synthesis of honeycomb-structured ZnO nanomaterials for photocatalytic degradation of methylene blue, *Mater. Lett.* 253 (2019) 30–33.
- [31] X. Yang, Y. Yang, B. Wang, T. Wang, Y. Wang, D. Meng, Synthesis and photocatalytic property of cubic phase CdS, *Solid State Sci.* 92 (2019) 31–35.
- [32] H. Pasdar, N. Elmi Fard, M. Rezvani, Fabrication of $\text{MoS}_2/\text{Bi}_2\text{S}_3$ heterostructure for photocatalytic degradation of Metronidazole and Cefalexin and antibacterial applications under NIR light: experimental and theoretical approach, *Appl. Phys. A* 129 (5) (2023) 380.
- [33] S.A.K. Vandani, M. Kalaei, M.G. Saravani, N.E. Fard, M. Rahmati, M. Kamani, Preparation of magnetic $\text{Fe}_3\text{O}_4/\text{MoO}_3/\text{MCM-22}$ photocatalyst and its study on metronidazole adsorption, degradation, and process optimization, *Russ. J. Phys. Chem. A* 97 (4) (2023) 618–632.
- [34] N.E. Fard, R. Fazaeli, Optimization of operating parameters in photocatalytic activity of visible light active Ag/TiO_2 nanoparticles, *Russ. J. Phys. Chem. A* 92 (2018) 2835–2846.
- [35] N.E. Fard, R. Fazaeli, R. Ghiasi, Band gap energies and photocatalytic properties of CdS and Ag/CdS nanoparticles for Azo dye degradation, *Chem. Eng. Technol.* 39 (1) (2016) 149–157.
- [36] D. Mukherjee, B. Van der Bruggen, B. Mandal, Advancements in visible light responsive MOF composites for photocatalytic decontamination of textile wastewater: a review, *Chemosphere* 295 (2022) 133835.
- [37] M. Ali, E. Pervaiz, T. Noor, O. Rabi, R. Zahra, M. Yang, Recent advancements in MOF-based catalysts for applications in electrochemical and photoelectrochemical water splitting: a review, *Int. J. Energy Res.* 45 (2) (2021) 1190–1226.
- [38] Y. Liu, D. Huang, M. Cheng, Z. Liu, C. Lai, C. Zhang, Q. Liang, Metal sulfide/MOF-based composites as visible-light-driven photocatalysts for enhanced hydrogen production from water splitting, *Coord. Chem. Rev.* 409 (2020) 213220.
- [39] G. Cai, P. Yan, L. Zhang, H.C. Zhou, H.L. Jiang, Metal-organic framework-based hierarchically porous materials: synthesis and applications, *Chem. Rev.* 121 (20) (2021) 12278–12326.
- [40] M.H. Yap, K.L. Fow, G.Z. Chen, Synthesis and applications of MOF-derived porous nanostructures, *Green Energy Environ.* 2 (3) (2017) 218–245.
- [41] P. Silva, S.M. Vilela, J.P. Tome, F.A.A. Paz, Multifunctional metal-organic frameworks: from academia to industrial applications, *Chem. Soc. Rev.* 44 (19) (2015) 6774–6803.
- [42] O.M. Yaghi, G. Li, H. Li, Selective binding and removal of guests in a microporous metal-organic framework, *Nature* 378 (6558) (1995) 703–706.
- [43] H. Furukawa, K.E. Cordova, M. O’Keeffe, O.M. Yaghi, The chemistry and applications of metal-organic frameworks, *Science* 341 (6149) (2013) 1230444.
- [44] S. Li, S. Shan, S. Chen, H. Li, Z. Li, Y. Liang, J. Li, Photocatalytic degradation of hazardous organic pollutants in water by Fe-MOFs and their composites: a review, *J. Environ. Chem. Eng.* 9 (5) (2021) 105967.
- [45] C.W. Huang, V.H. Nguyen, S.R. Zhou, S.Y. Hsu, J.X. Tan, K.C.W. Wu, Metal-organic frameworks: preparation and applications in highly efficient heterogeneous photocatalysis, *Sustain. Energy Fuels* 4 (2) (2020) 504–521.

- [46] S.A. Younis, E.E. Kwon, M. Qasim, K.H. Kim, T. Kim, D. Kukkar, I. Ali, Metal-organic framework as a photocatalyst: progress in modulation strategies and environmental/energy applications, *Prog. Energy Combust. Sci.* 81 (2020) 100870.
- [47] Y. Shan, L. Chen, H. Pang, Q. Xu, Metal-organic framework-based hybrid frameworks, *Small Structures* 2 (2) (2021) 2000078.
- [48] I. Ashraf, S. Rizwan, M. Iqbal, A comprehensive review on the synthesis and energy applications of nano-structured metal nitrides, *Frontiers in Materials* 7 (2020) 181.
- [49] A. Ray, S. Sultana, S.P. Tripathy, K. Parida, Aggrandizing the photoactivity of ZnO nanorods toward N₂ reduction and H₂ evolution through facile in situ coupling with Ni x P y, *ACS Sustain. Chem. Eng.* 9 (18) (2021) 6305–6317.
- [50] N. Elmi Fard, R. Fazaeli, M. Yousefi, S. Abdolmohammadi, Oxidation of carbazole by shape-controllable Cu₂O on MWW catalysis, *Appl. Phys. A* 125 (9) (2019) 632.
- [51] N.E. Fard, R. Fazaeli, M. Yousefi, S. Abdolmohammadi, Morphology-controlled synthesis of CuO, CuO rod/MWW composite for advanced oxidation of indole and benzothiophene, *ChemistrySelect* 4 (33) (2019) 9529–9539.
- [52] N.E. Fard, R. Fazaeli, M. Yousefi, S. Abdolmohammadi, Oxidative desulfurization of dibenzothiophene using M/TiO₂/MWW (M= Cu, Ag, and Au) composite, *Russ. J. Phys. Chem. A* 95 (Suppl 1) (2021) S23–S32.
- [53] D. Kandi, S. Martha, A. Thirumurugan, K.M. Parida, Modification of BiOI microplates with CdS QDs for enhancing stability, optical property, electronic behavior toward rhodamine B decolorization, and photocatalytic hydrogen evolution, *J. Phys. Chem. C* 121 (9) (2017) 4834–4849.
- [54] J. Ge, Y. Zhang, S.J. Park, Recent advances in carbonaceous photocatalysts with enhanced photocatalytic performances: a mini review, *Materials* 12 (12) (2019) 1916.
- [55] G. Swain, S. Sultana, K. Parida, Constructing a novel surfactant-free MoS₂ nanosheet modified MgIn₂S₄ marigold microflower: an efficient visible-light driven 2D-2D pn heterojunction photocatalyst toward HER and pH regulated NRR, *ACS Sustain. Chem. Eng.* 8 (12) (2020) 4848–4862.
- [56] N.E. Fard, R. Fazaeli, A novel kinetic approach for photocatalytic degradation of azo dye with CdS and Ag/CdS nanoparticles fixed on a cement bed in a continuous-flow photoreactor, *Int. J. Chem. Kinet.* 48 (11) (2016) 691–701.
- [57] A. Ray, S. Sultana, L. Paramanik, K.M. Parida, Recent advances in phase, size, and morphology-oriented nanostructured nickel phosphide for overall water splitting, *J. Mater. Chem. A* 8 (37) (2020) 19196–19245.
- [58] D.P. Sahoo, S. Patnaik, K. Parida, Construction of a Z-scheme dictated WO₃-X/Ag/ZnCr LDH synergistically visible light-induced photocatalyst towards tetracycline degradation and H₂ evolution, *ACS Omega* 4 (12) (2019) 14721–14741.
- [59] L. Acharya, S. Nayak, S.P. Pattnaik, R. Acharya, K. Parida, Resurrection of boron nitride in pn type-II boron nitride/B-doped-g-C₃N₄ nanocomposite during solid-state Z-scheme charge transfer path for the degradation of tetracycline hydrochloride, *J. Colloid Interface Sci.* 566 (2020) 211–223.
- [60] V.M. Avargani, S. Zendejboudi, S. Osfour, A. Rostami, Performance evaluation of a solar nano-photocatalytic reactor for wastewater treatment applications: reaction kinetics, CFD, and scale-up perspectives, *J. Clean. Prod.* 421 (2023) 138240.
- [61] T. Xia, Y. Lin, W. Li, M. Ju, Photocatalytic degradation of organic pollutants by MOFs based materials: a review, *Chin. Chem. Lett.* 32 (10) (2021) 2975–2984.
- [62] L. Fang, Z. Liu, C. Zhou, Y. Guo, Y. Feng, M. Yang, Degradation mechanism of methylene blue by H₂O₂ and synthesized carbon nanodots/graphitic carbon nitride/Fe (II) composite, *J. Phys. Chem. C* 123 (44) (2019) 26921–26931.
- [63] M.A. Abid, D.A. Abid, W.J. Aziz, T.M. Rashid, Iron oxide nanoparticles synthesized using garlic and onion peel extracts rapidly degrade methylene blue dye, *Phys. B Condens. Matter* 622 (2021) 413277.
- [64] M.A. Abid, D.A. Abid, W.J. Aziz, T.M. Rashid, Iron oxide nanoparticles synthesized using garlic and onion peel extracts rapidly degrade methylene blue dye, *Phys. B Condens. Matter* 622 (2021) 413277.
- [65] A. Rehman, A. Daud, M.F. Warsi, I. Shakir, P.O. Agboola, M.I. Sarwar, S. Zulfiqar, Nanostructured maghemite and magnetite and their nanocomposites with graphene oxide for photocatalytic degradation of methylene blue, *Mater. Chem. Phys.* 256 (2020) 123752.
- [66] A. Farhan, M. Zahid, N. Tahir, A. Mansha, M. Yaseen, G. Mustafa, I. Shahid, Investigation of boron-doped graphene oxide anchored with copper sulphide flowers as visible light active photocatalyst for methylene blue degradation, *Sci. Rep.* 13 (1) (2023) 9497.
- [67] R.K. Sithole, L.F. Machogo, M.J. Moloto, S.S. Gqoba, K.P. Mubiayi, J. Van Wyk, N. Moloto, One-step synthesis of Cu₃N, Cu₂S and Cu₉S₅ and photocatalytic degradation of methyl orange and methylene blue, *J. Photochem. Photobiol. Chem.* 397 (2020) 112577.
- [68] A.S. Eltaweil, E.M. Abd El-Monaem, G.M. El-Subruiti, M.M. Abd El-Latif, A.M. Omer, Fabrication of UiO-66/MIL-101 (Fe) binary MOF/carboxylated-GO composite for adsorptive removal of methylene blue dye from aqueous solutions, *RSC Adv.* 10 (32) (2020) 19008–19019.
- [69] T. Saemian, M.H. Sadr, M.T. Yarak, M. Gharagozlou, B. Soltani, Synthesis and characterization of CoFe₂O₄/SiO₂/Cu-MOF for degradation of methylene blue through catalytic sono-Fenton-like reaction, *Inorg. Chem. Commun.* 138 (2022) 109305.
- [70] M. Khajeh, A.R. Oveisi, A. Barkhordar, M. Rakhshanipour, H. Sargazi-Avval, Ternary NiCuZr layered double hydroxide@ MIL-101 (Fe)-NH₂ metal-organic framework for photocatalytic degradation of methylene blue, *Journal of Nanostructure in Chemistry* 12 (1) (2022) 105–115.
- [71] W. Chen, L. Du, C. Wu, Hydrothermal synthesis of MOFs, in: *Metal-Organic Frameworks for Biomedical Applications*, Woodhead Publishing, 2020, pp. 141–157.
- [72] S.H. Feng, G.H. Li, Hydrothermal and solvothermal syntheses, in: *Modern Inorganic Synthetic Chemistry*, Elsevier, 2017, pp. 73–104.
- [73] B. Yang, J. Huang, J. Tong, H. Peng, Y. Xiang, M. Ruan, W. Xiong, Microwave synthesis of Fe–Cu diatomic active center MOF: synergistic cyclic catalysis of persulfate for degrading norfloxacin, *Environ. Sci.: Nano* 10 (10) (2023) 2778–2789.
- [74] K. Yu, Y.R. Lee, J.Y. Seo, K.Y. Baek, Y.M. Chung, W.S. Ahn, Sonochemical synthesis of Zr-based porphyrinic MOF-525 and MOF-545: enhancement in catalytic and adsorption properties, *Microporous Mesoporous Mater.* 316 (2021) 110985.
- [75] J. Yang, Y.W. Yang, Metal-organic frameworks for biomedical applications, *Small* 16 (10) (2020) 1906846.
- [76] M. Ahmadi, M. Ebrahimi, M.A. Shahbazi, R. Keçili, F. Ghorbani-Bidkorbeh, Microporous metal-organic frameworks: synthesis and applications, *J. Ind. Eng. Chem.* 115 (2022) 1–11.
- [77] W. Zheng, X. Hao, L. Zhao, W. Sun, Controllable preparation of nanoscale metal-organic frameworks by ionic liquid microemulsions, *Ind. Eng. Chem. Res.* 56 (20) (2017) 5899–5905.
- [78] T. Xia, Y. Lin, W. Li, M. Ju, Photocatalytic degradation of organic pollutants by MOFs based materials: a review, *Chin. Chem. Lett.* 32 (10) (2021) 2975–2984.
- [79] M. Safaei, M.M. Foroughi, N. Ebrahimpour, S. Jahani, A. Omid, M. Khatami, A review on metal-organic frameworks: synthesis and applications, *TrAC, Trends Anal. Chem.* 118 (2019) 401–425.
- [80] M. Rubio-Martinez, C. Avci-Camur, A.W. Thornton, I. Imaz, D. Maspocho, M.R. Hill, New synthetic routes towards MOF production at scale, *Chem. Soc. Rev.* 46 (11) (2017) 3453–3480.
- [81] Z.W. Zhu, Q.R. Zheng, Investigation of cryo-adsorption hydrogen storage capacity of rapidly synthesized MOF-5 by mechanochemical method, *Int. J. Hydrogen Energy* 48 (13) (2023) 5166–5174.
- [82] E.M.C. Morales, M.A. Méndez-Rojas, L.M. Torres-Martínez, L.F. Garay-Rodríguez, I. López, I.E. Uflyand, B.I. Kharisov, Ultrafast synthesis of HKUST-1 nanoparticles by solvothermal method: properties and possible applications, *Polyhedron* 210 (2021) 115517.
- [83] H. Sugiura, H. Kajiro, H. Kanoh, Calorimetric study of the CO₂ gate sorption of elastic layer-structured metal-organic frameworks (ELM-11 and ELM-12), *Colloids Surf. A Physicochem. Eng. Asp.* 651 (2022) 129745.
- [84] S.H. Mosavi, R. Zare-Dorabei, M. Bereyhi, Microwave-assisted synthesis of metal-organic framework MIL-47 for effective adsorptive removal of dibenzothiophene from model fuel, *J. Iran. Chem. Soc.* 18 (2021) 709–717.
- [85] E. Yilmaz, E. Sert, F.S. Atalay, Synthesis, characterization of a metal organic framework: MIL-53 (Fe) and adsorption mechanisms of methyl red onto MIL-53 (Fe), *J. Taiwan Inst. Chem. Eng.* 65 (2016) 323–330.
- [86] S. Darvishi, S. Javanbakht, A. Heydari, F. Kazeminava, P. Gholizadeh, M. Mahdipour, A. Shaabani, Ultrasound-assisted synthesis of MIL-88 (Fe) coordinated to carboxymethyl cellulose fibers: a safe carrier for highly sustained release of tetracycline, *Int. J. Biol. Macromol.* 181 (2021) 937–944.
- [87] M. Forghani, A. Azizi, M.J. Livani, L.A. Kafshgari, Adsorption of lead (II) and chromium (VI) from aqueous environment onto metal-organic framework MIL-100 (Fe): synthesis, kinetics, equilibrium and thermodynamics, *J. Solid State Chem.* 291 (2020) 121636.

- [88] M. Zou, M. Dong, T. Zhao, Advances in metal-organic frameworks MIL-101 (Cr), *Int. J. Mol. Sci.* 23 (16) (2022) 9396.
- [89] D. Hidayat, W.W. Lestari, D. Dendy, F. Khoerunnisa, M. Handayani, E.H. Sanjaya, T. Gunawan, Adsorption studies of anionic and cationic dyes on MIL-100 (Cr) synthesized using facile and green mechanochemical method, *J. Inorg. Organomet. Polym. Mater.* (2023) 1–14.
- [90] J. Guasch, P.D. Dietzel, P. Collier, N. Acerbi, The effect of solvent and Temperature in the synthesis of CPO-27-Ni by reflux, *Microporous Mesoporous Mater.* 203 (2015) 238–244.
- [91] M. Nasrabadi, M.A. Ghasemzadeh, M.R.Z. Monfared, The preparation and characterization of UiO-66 metal-organic frameworks for the delivery of the drug ciprofloxacin and an evaluation of their antibacterial activities, *New J. Chem.* 43 (40) (2019) 16033–16040.
- [92] M. Ikram, H. Lv, Z. Liu, K. Shi, Y. Gao, Hydrothermally derived p-n MoS₂-ZnO from p-p MoS₂-ZIF-8 for an efficient detection of NO₂ at room temperature, *J. Mater. Chem. A* 9 (26) (2021) 14722–14730.
- [93] S. Gaikwad, S.-J. Kim, S. Han, Novel Metal-Organic Framework of UTSA-16 (Zn) Synthesized by a Microwave Method: Outstanding Performance for CO₂ Capture with Improved Stability to Acid Gases, *Journal of Industrial and Engineering Chemistry* 87 (2020) 250–263.
- [94] D.D. Kachhadiya, A.V. Sonawane, Z.V.P. Murthy, Metal-organic frameworks (MOFs) characterization using different analytical methods, in: *Metal-Organic Frameworks (MOFs) as Catalysts*, Springer Nature Singapore, Singapore, 2022, pp. 165–180.
- [95] V. Russo, M. Hmoudah, F. Broccoli, M.R. Iesce, O.S. Jung, M. Di Serio, Applications of metal organic frameworks in wastewater treatment: a review on adsorption and photodegradation, *Frontiers in Chemical Engineering* 2 (2020) 581487.
- [96] S. Ghafoori, M. Omar, N. Koutahzadeh, S. Zendejboudi, R.N. Malhas, New advancements, challenges, and future needs on treatment of oilfield produced water: a state-of-the-art review, *Sep. Purif. Technol.* 289 (2022) 120652.
- [97] S.S. Fekra, N.E. Fard, R. Fazaeli, Photocatalytic degradation of antibiotic norfloxacin aqueous solution by Ce/Bi₂WO₆: optimization and simulation of process by RSM, *Russ. J. Appl. Chem.* 94 (6) (2021) 824–834.
- [98] Y. Zhang, B. Zhou, H. Chen, R. Yuan, Heterogeneous photocatalytic oxidation for the removal of organophosphorus pollutants from aqueous solutions: a review, *Sci. Total Environ.* 856 (2023) 159048.
- [99] Y. Pan, Y. Zhang, Y. Huang, Y. Jia, L. Chen, Enhanced photocatalytic oxidation degradability for real cyanide wastewater by designing photocatalyst GO/TiO₂/ZSM-5: performance and mechanism research, *Chem. Eng. J.* 428 (2022) 131257.
- [100] A. Azanaw, B. Birilie, B. Teshome, M. Jemberie, Textile effluent treatment methods and eco-friendly resolution of textile wastewater, *Case Studies in Chemical and Environmental Engineering* 6 (2022) 100230.
- [101] A. Pattnaik, J.N. Sahu, A.K. Poonia, P. Ghosh, Current perspective of nano-engineered metal oxide based photocatalysts in advanced oxidation processes for degradation of organic pollutants in wastewater, *Chem. Eng. Res. Des.* 190 (2023) 667–686.
- [102] S. Feijoo, M. Kamali, R. Dewil, A review of wastewater treatment technologies for the degradation of pharmaceutically active compounds: carbamazepine as a case study, *Chem. Eng. J.* 455 (2023) 140589.
- [103] M. Gharagozlu, N.E. Fard, M. Ghahari, M.T. Yarak, Bimetal Cu/Ni-BTC@ SiO₂ metal-organic framework as high performance photocatalyst for degradation of azo dyes under visible light irradiation, *Environ. Res.* 256 (2024) 119229.
- [104] Z.U. Zango, K.S. Khoo, A. Garba, H.A. Kadir, F. Usman, M.U. Zango, J.W. Lim, A review on superior advanced oxidations and photocatalytic degradation techniques for perfluorooctanoic acid (PFOA) elimination from wastewater, *Environ. Res.* 221 (2023) 115326.
- [105] G. Sriram, A. Bendre, E. Mariappan, T. Altalhi, M. Kigga, Y.C. Ching, M. Kurkuri, Recent trends in the application of metal-organic frameworks (MOFs) for the removal of toxic dyes and their removal mechanism—a review, *Sustainable Materials and Technologies* 31 (2022) e00378.
- [106] S. Gautam, H. Agrawal, M. Thakur, A. Akbari, H. Sharda, R. Kaur, M. Amini, Metal oxides and metal organic frameworks for the photocatalytic degradation: a review, *J. Environ. Chem. Eng.* 8 (3) (2020) 103726.
- [107] S.W. Lv, J.M. Liu, C.Y. Li, H. Ma, Z.H. Wang, N. Zhao, S. Wang, Fabrication of Fe₃O₄@ UiO-66-SO₃ H core-shell functional adsorbents for highly selective and efficient removal of organic dyes, *New J. Chem.* 43 (20) (2019) 7770–7777.
- [108] S. Yang, X. Li, G. Zeng, M. Cheng, D. Huang, Y. Liu, G. Zhang, Materials Institute Lavoisier (MIL) based materials for photocatalytic applications, *Coord. Chem. Rev.* 438 (2021) 213874.
- [109] Y.B. Huang, J. Liang, X.S. Wang, R. Cao, Multifunctional metal-organic framework catalysts: synergistic catalysis and tandem reactions, *Chem. Soc. Rev.* 46 (1) (2017) 126–157.
- [110] C.C. Wang, X.H. Yi, P. Wang, Powerful combination of MOFs and C₃N₄ for enhanced photocatalytic performance, *Appl. Catal. B Environ.* 247 (2019) 24–48.
- [111] S.W. Lv, J.M. Liu, F.E. Yang, C.Y. Li, S. Wang, A novel photocatalytic platform based on the newly-constructed ternary composites with a double pn heterojunction for contaminants degradation and bacteria inactivation, *Chem. Eng. J.* 409 (2021) 128269.
- [112] X. Zhao, J. Li, X. Li, P. Huo, W. Shi, Design of metal-organic frameworks (MOFs)-based photocatalyst for solar fuel production and photo-degradation of pollutants, *Chin. J. Catal.* 42 (6) (2021) 872–903.
- [113] S.W. Lv, Y. Cong, X. Chen, W. Wang, L. Che, Developing fine-tuned metal-organic frameworks for photocatalytic treatment of wastewater: a review, *Chem. Eng. J.* 433 (2022) 133605.
- [114] S.W. Lv, J.M. Liu, N. Zhao, C.Y. Li, F.E. Yang, Z.H. Wang, S. Wang, MOF-derived CoFe₂O₄/Fe₂O₃ embedded in g-C₃N₄ as high-efficient Z-scheme photocatalysts for enhanced degradation of emerging organic pollutants in the presence of persulfate, *Sep. Purif. Technol.* 253 (2020) 117413.
- [115] C. Candia-Onfray, S. Rojas, M.V.B. Zanoni, R. Salazar, An updated review of metal-organic framework materials in photo (electro) catalytic applications: from CO₂ reduction to wastewater treatments, *Curr. Opin. Electrochem.* 26 (2021) 100669.
- [116] T. Rasheed, M.T. Anwar, Metal organic frameworks as self-sacrificing modalities for potential environmental catalysis and energy applications: challenges and perspectives, *Coord. Chem. Rev.* 480 (2023) 215011.
- [117] T. Wu, X. Liu, Y. Liu, M. Cheng, Z. Liu, G. Zeng, Q. He, Application of QD-MOF composites for photocatalysis: energy production and environmental remediation, *Coord. Chem. Rev.* 403 (2020) 213097.
- [118] H. Lin, Y. Xu, B. Wang, D.S. Li, T. Zhou, J. Zhang, Postsynthetic modification of metal-organic frameworks for photocatalytic applications, *Small Structures* 3 (5) (2022) 2100176.
- [119] S. Chowdhury, P. Sharma, K. Kundu, P.P. Das, P. Rathi, P.F. Siril, Systematic thiol decoration in a redox-active UiO-66-(SH)₂ metal-organic framework: a case study under oxidative and reductive conditions, *Inorg. Chem.* 62 (9) (2023) 3875–3885.
- [120] C. Gomes Silva, I. Luz, F.X. Llabres i Xamena, A. Corma, H. García, Water stable Zr-benzenedicarboxylate metal-organic frameworks as photocatalysts for hydrogen generation, *Chem.–Eur. J.* 16 (36) (2010) 11133–11138.
- [121] S.W. Lv, J.M. Liu, N. Zhao, C.Y. Li, Z.H. Wang, S. Wang, Benzothiadiazole functionalized Co-doped MIL-53-NH₂ with electron deficient units for enhanced photocatalytic degradation of bisphenol A and ofloxacin under visible light, *J. Hazard Mater.* 387 (2020) 122011.
- [122] X. Jia, F. Wang, X. Xu, C. Liu, L. Zhang, S. Jiao, G. Yu, Highly efficient photocatalytic degradation of tetracycline by modifying UiO-66 via different regulation strategies, *ACS Omega* 8 (30) (2023) 27375–27385.
- [123] L. Yin, D. Wang, X. Li, Y. He, X. Liu, Y. Xu, H. Chen, One-pot synthesis of oxygen-vacancy-rich Cu-doped UiO-66 for collaborative adsorption and photocatalytic degradation of ciprofloxacin, *Sci. Total Environ.* 815 (2022) 151962.
- [124] R. Li, T. Chen, J. Lu, H. Hu, H. Zheng, P. Zhu, X. Pan, Metal-organic frameworks doped with metal ions for efficient sterilization: enhanced photocatalytic activity and photothermal effect, *Water Res.* 229 (2023) 119366.
- [125] L. Yin, D. Wang, X. Li, Y. He, X. Liu, Y. Xu, H. Chen, One-pot synthesis of oxygen-vacancy-rich Cu-doped UiO-66 for collaborative adsorption and photocatalytic degradation of ciprofloxacin, *Sci. Total Environ.* 815 (2022) 151962.
- [126] Y. Liu, G. Zhu, J. Gao, R. Zhu, M. Hojamberdiev, C. Wang, P. Liu, A novel synergy of Er³⁺/Fe³⁺ co-doped porous Bi₂O₇ microspheres with enhanced photocatalytic activity under visible-light irradiation, *Appl. Catal. B Environ.* 205 (2017) 421–432.
- [127] R. Kaur, A. Kaur, R. Kaur, S. Singh, M.S. Bhatti, A. Umar, S.K. Kansal, Cu-BTC metal organic framework (MOF) derived Cu-doped TiO₂ nanoparticles and their use as visible light active photocatalyst for the decomposition of ofloxacin (OFX) antibiotic and antibacterial activity, *Adv. Powder Technol.* 32 (5) (2021) 1350–1361.

- [128] M. Chen, X. Wei, L. Zhao, Y. Huang, S.C. Lee, W. Ho, K. Chen, Novel N/carbon quantum dot modified MIL-125 (Ti) composite for enhanced visible-light photocatalytic removal of NO, *Ind. Eng. Chem. Res.* 59 (14) (2020) 6470–6478.
- [129] Y. Zhang, G. Li, Q. Guo, CdSe QDs@ Fe-based metal organic framework composites for improved photocatalytic RhB degradation under visible light, *Microporous Mesoporous Mater.* 324 (2021) 111291.
- [130] G. Zhang, S. Chen, Y. Yang, Y. Liu, L. Lei, X. Liu, M. Cheng, Boron nitride quantum dots decorated MIL-100 (Fe) for boosting the photo-generated charge separation in photocatalytic refractory antibiotics removal, *Environ. Res.* 202 (2021) 111661.
- [131] S.W. Lv, Y. Cong, X. Chen, W. Wang, L. Che, Developing fine-tuned metal–organic frameworks for photocatalytic treatment of wastewater: a review, *Chem. Eng. J.* 433 (2022) 133605.
- [132] Y.J. Lai, D.J. Lee, Pollutant degradation with mediator Z-scheme heterojunction photocatalyst in water: a review, *Chemosphere* 282 (2021) 131059.
- [133] J.T. Ren, K. Yuan, K. Wu, L. Zhou, Y.W. Zhang, A robust CdS/In₂O₃ hierarchical heterostructure derived from a metal–organic framework for efficient visible-light photocatalytic hydrogen production, *Inorg. Chem. Front.* 6 (2) (2019) 366–375.
- [134] P. Behera, S. Subudhi, S.P. Tripathy, K. Parida, MOF derived nano-materials: a recent progress in strategic fabrication, characterization and mechanistic insight towards divergent photocatalytic applications, *Coord. Chem. Rev.* 456 (2022) 214392.
- [135] B. Hu, J.Y. Yuan, J.Y. Tian, M. Wang, X. Wang, L. He, C.S. Liu, Co/Fe-bimetallic organic framework-derived carbon-incorporated cobalt–ferric mixed metal phosphide as a highly efficient photocatalyst under visible light, *J. Colloid Interface Sci.* 531 (2018) 148–159.
- [136] T.S. Natarajan, K.R. Thampi, R.J. Tayade, Visible light driven redox-mediator-free dual semiconductor photocatalytic systems for pollutant degradation and the ambiguity in applying Z-scheme concept, *Appl. Catal. B Environ.* 227 (2018) 296–311.
- [137] S. Dissegna, K. Epp, W.R. Heinz, G. Kieslich, R.A. Fischer, Defective metal-organic frameworks, *Adv. Mater.* 30 (37) (2018) 1704501.
- [138] D.S. Sholl, R.P. Lively, Defects in metal–organic frameworks: challenge or opportunity? *J. Phys. Chem. Lett.* 6 (17) (2015) 3437–3444.
- [139] Y.J. Lai, D.J. Lee, Solid mediator Z-scheme heterojunction photocatalysis for pollutant oxidation in water: principles and synthesis perspectives, *J. Taiwan Inst. Chem. Eng.* 125 (2021) 88–114.
- [140] F. Wang, T. He, Y. Gao, Y. Li, S. Cui, H. Huang, J. Yang, Z-scheme heterojunction Bi₂MoO₆/NH₂-UiO-66 (Zr/Ce) for efficient photocatalytic degradation of oxytetracycline: pathways and mechanism, *Sep. Purif. Technol.* 325 (2023) 124596.
- [141] X. Ma, L. Wang, Q. Zhang, H.L. Jiang, Switching on the photocatalysis of metal–organic frameworks by engineering structural defects, *Angew. Chem. Int. Ed.* 58 (35) (2019) 12175–12179.
- [142] R. Xu, Q. Zhang, J.Y. Wang, D. Liu, J. Wang, Z.L. Wang, Direct current triboelectric cell by sliding an n-type semiconductor on a p-type semiconductor, *Nano Energy* 66 (2019) 104185.
- [143] A. Lasia, A. Lasia, Semiconductors and Mott-Schottky plots. *Electrochemical Impedance Spectroscopy and its Applications*, 2014, pp. 251–255.
- [144] Y. Li, S. Liu, R. Liu, J. Pan, X. Li, J. Zhang, S. Zhu, Nanoarchitectonics on Z-scheme and Mott–Schottky heterostructure for photocatalytic water oxidation via dual-cascade charge-transfer pathways, *Nanoscale Adv* 5 (2023) 3386–3395.
- [145] S. Bargoziadeh, M. Tasviri, S. Shekarabi, H. Daneshgar, Magnetic BiFeO₃ decorated UiO-66 as ap–n heterojunction photocatalyst for simultaneous degradation of a binary mixture of anionic and cationic dyes, *New J. Chem.* 44 (30) (2020) 13083–13092.
- [146] W. Zhang, D. Liu, Z. Mu, X. Zhang, G. Dong, L. Bai, Z. Zhang, Insight into the novel Z-scheme ZIF67/WO₃ heterostructure for improved photocatalytic degradation of methylene blue under visible light, *J. Inorg. Organomet. Polym. Mater.* 33 (1) (2023) 90–104.
- [147] H. Sepehrmansourie, H. Alamgholiloo, N.N. Pesyan, M.A. Zolfigol, A MOF-on-MOF strategy to construct double Z-scheme heterojunction for high-performance photocatalytic degradation, *Appl. Catal. B Environ.* 321 (2023) 122082.
- [148] F.-Z. Chen, Y.-J. Li, M. Zhou, X.-X. Gong, Y. Gao, G. Cheng, S.-B. Ren, D.-M. Han, Smart multifunctional direct Z-scheme In₂S₃@PCN-224 heterojunction for simultaneous detection and photodegradation towards antibiotic pollutants, *Appl. Catal. B Environ.* 328 (2023) 122517.
- [149] X. Zheng, Y. Li, J. Yang, S. Cui, Z-Scheme heterojunction Ag/NH₂-MIL-125 (Ti)/CdS with enhanced photocatalytic activity for ketoprofen degradation: mechanism and intermediates, *Chem. Eng. J.* 422 (2021) 130105.
- [150] C. Liu, P. Wang, Y. Qiao, G. Zhou, Self-assembled Bi₂SeO₅/rGO/MIL-88A Z-scheme heterojunction boosting carrier separation for simultaneous removal of Cr (VI) and chloramphenicol, *Chem. Eng. J.* 431 (2022) 133289.
- [151] Y. Liu, Y. Zhou, Q. Tang, Q. Li, S. Chen, Z. Sun, H. Wang, A direct Z-scheme Bi₂WO₆/NH₂-UiO-66 nanocomposite as an efficient visible-light-driven photocatalyst for NO removal, *RSC Adv.* 10 (3) (2020) 1757–1768.
- [152] S. Bargoziadeh, M. Tasviri, S. Shekarabi, H. Daneshgar, Magnetic BiFeO₃ decorated UiO-66 as ap–n heterojunction photocatalyst for simultaneous degradation of a binary mixture of anionic and cationic dyes, *New J. Chem.* 44 (30) (2020) 13083–13092.
- [153] Z. Lin, Y. Wu, X. Jin, D. Liang, Y. Jin, S. Huang, Z. Wang, H. Liu, P. Chen, W. Lv, G. Liu, Facile synthesis of direct Z-scheme UiO-66-NH₂/PhC₂Cu heterojunction with ultrahigh redox potential for enhanced photocatalytic Cr(VI) reduction and NOR degradation, *J Hazard Mater* 443 (2023) 130195.
- [154] Y. Ma, X. Qian, M. Arif, J. Xia, H. Fan, J. Luo, H. Chen, Z-scheme Bi₄O₅Br₂/MIL-88B (Fe) heterojunction for boosting visible light catalytic oxidation of tetracycline hydrochloride, *Appl. Surf. Sci.* 611 (2023) 155667.
- [155] K. Zhang, Y. Fu, D. Hao, J. Guo, B.J. Ni, B. Jiang, Q. Wang, Fabrication of CN75/NH₂-MIL-53 (Fe) pn heterojunction with wide spectral response for efficiently photocatalytic Cr (VI) reduction, *J. Alloys Compd.* 891 (2022) 161994.
- [156] J. Abdul Nasir, A. Munir, N. Ahmad, T.U. Haq, Z. Khan, Z. Rehman, Photocatalytic Z-scheme overall water splitting: recent advances in theory and experiments, *Adv. Mater.* 33 (52) (2021) 2105195.
- [157] H. Luo, Z. Zeng, G. Zeng, C. Zhang, R. Xiao, D. Huang, S. Tian, Recent progress on metal-organic frameworks based-and derived-photocatalysts for water splitting, *Chem. Eng. J.* 383 (2020) 123196.
- [158] M. Liu, L.Z. Qiao, B.B. Dong, S. Guo, S. Yao, C. Li, T.B. Lu, Photocatalytic coproduction of H₂ and industrial chemical over MOF-derived direct Z-scheme heterostructure, *Appl. Catal. B Environ.* 273 (2020) 119066.
- [159] S. He, Q. Rong, H. Niu, Y. Cai, Platform for molecular-material dual regulation: a direct Z-scheme MOF/COF heterojunction with enhanced visible-light photocatalytic activity, *Appl. Catal. B Environ.* 247 (2019) 49–56.
- [160] L. Cheng, M. Xie, Y. Sun, H. Liu, Bi₂WO₆-wrapped 2D Ni-MOF sheets with significantly improved photocatalytic activity by a direct Z-scheme electron transfer, *J. Alloys Compd.* 896 (2022) 163055.
- [161] F. Wu, C. Zhou, G. Tai, Y. Ma, X. Yang, Y. Pan, G. Wu, ZIF-67/BiOCl Z-scheme heterojunction photocatalyst for photodegradation of organic dyes and antibiotics, *ACS Appl. Nano Mater.* 6 (19) (2023) 17814–17825.
- [162] Y. Pan, X. Hu, D. Shen, Z. Li, R. Chen, Y. Li, M. Bao, Facile construction of Z-scheme Fe-MOF@ BiOBr/M– CN heterojunction for efficient degradation of ciprofloxacin, *Sep. Purif. Technol.* 295 (2022) 121216.
- [163] Y. Chai, Y. Zhang, L. Wang, Y. Du, B. Wang, N. Li, L. Ou, In situ one-pot construction of MOF/hydrogel composite beads with enhanced wastewater treatment performance, *Sep. Purif. Technol.* 295 (2022) 121225.
- [164] H. Sepehrmansourie, H. Alamgholiloo, N.N. Pesyan, M.A. Zolfigol, A MOF-on-MOF strategy to construct double Z-scheme heterojunction for high-performance photocatalytic degradation, *Appl. Catal. B Environ.* 321 (2023) 122082.
- [165] F. Mu, Q. Cai, H. Hu, J. Wang, Y. Wang, S. Zhou, Y. Kong, Construction of 3D hierarchical microarchitectures of Z-scheme UiO-66-(COOH)₂/ZnIn₂S₄ hybrid decorated with non-noble MoS₂ cocatalyst: a highly efficient photocatalyst for hydrogen evolution and Cr (VI) reduction, *Chem. Eng. J.* 384 (2020) 123352.
- [166] N. Chang, Y.R. Chen, F. Xie, Y.P. Liu, H.T. Wang, A promising Z-scheme heterojunction via loading Ag/AgCl into porous Co₃O₄ derived from ZIF-67 for visible light driven photocatalysis, *Microporous Mesoporous Mater.* 307 (2020) 110530.
- [167] N. Chang, Y.R. Chen, F. Xie, Y.P. Liu, H.T. Wang, Facile construction of Z-scheme AgCl/Ag-doped-ZIF-8 heterojunction with narrow band gaps for efficient visible-light photocatalysis, *Colloids Surf. A Physicochem. Eng. Asp.* 616 (2021) 126351.
- [168] J. Ren, S. Lv, S. Wang, M. Bao, X. Zhang, Y. Gao, J. Ke, Construction of efficient g-C₃N₄/NH₂-UiO-66 (Zr) heterojunction photocatalysts for wastewater purification, *Sep. Purif. Technol.* 274 (2021) 118973.

- [169] X. Zhang, H. Zhou, W. Cao, C. Chen, C. Jiang, Y. Wang, Preparation and mechanism investigation of $\text{Bi}_2\text{WO}_6/\text{UiO}-66\text{-NH}_2$ Z-scheme heterojunction with enhanced visible light catalytic activity, *Inorg. Chem. Commun.* 120 (2020) 108162.
- [170] H. Zhang, Q. Meng, H. Li, G. Wu, K. Li, J. Xu, H. Hou, BiOI nanoparticle/PCN-222 heterojunctions as self-decontaminating photocatalysts with efficient tetracycline visible-light degradation, *CrystEngComm* 24 (43) (2022) 7611–7619.
- [171] N.T. Tran, M.K. Nguyen, The degradation of organic dye contaminants in wastewater and solution from highly visible light responsive ZIF-67 monodisperse photocatalyst, *J. Solid State Chem.* 300 (2021) 122287.
- [172] B. Xue, L. Du, J. Jin, H. Meng, J. Mi, In situ growth of MIL-88A into polyacrylate and its application in highly efficient photocatalytic degradation of organic pollutants in water, *Appl. Surf. Sci.* 564 (2021) 150404.
- [173] Y. Gao, S. Li, Y. Li, L. Yao, H. Zhang, Accelerated photocatalytic degradation of organic pollutant over metal-organic framework MIL-53 (Fe) under visible LED light mediated by persulfate, *Appl. Catal. B Environ.* 202 (2017) 165–174.
- [174] L. Li, X. Yu, L. Xu, Y. Zhao, Fabrication of a novel type visible-light-driven heterojunction photocatalyst: metal-porphyrinic metal organic framework coupled with $\text{PW}_{12}/\text{TiO}_2$, *Chem. Eng. J.* 386 (2020) 123955.
- [175] Y.Y. Tong, Y.F. Li, L. Sun, R. Yang, S. Zhang, Y. Fu, R. Chen, The prominent photocatalytic activity with the charge transfer in the organic ligand for $[\text{Zn}_4\text{O}(\text{BDC})_3]$ MOF-5 decorated Ag_3PO_4 hybrids, *Sep. Purif. Technol.* 250 (2020) 117142.
- [176] N. Askari, M. Beheshti, D. Mowla, M. Farhadian, Fabrication of $\text{CuWO}_4/\text{Bi}_2\text{S}_3/\text{ZIF67}$ MOF: a novel double Z-scheme ternary heterostructure for boosting visible-light photodegradation of antibiotics, *Chemosphere* 251 (2020) 126453.
- [177] X. Lei, J. Wang, Y. Shi, W. Yao, Q. Wu, Q. Wu, R. Zou, Constructing novel red phosphorus decorated iron-based metal organic framework composite with efficient photocatalytic performance, *Appl. Surf. Sci.* 528 (2020) 146963.
- [178] S.W. Lv, J.M. Liu, N. Zhao, C.Y. Li, Z.H. Wang, S. Wang, Benzothiadiazole functionalized Co-doped MIL-53- NH_2 with electron deficient units for enhanced photocatalytic degradation of bisphenol A and ofloxacin under visible light, *J. Hazard Mater.* 387 (2020) 122011.
- [179] W. Cao, Y. Yuan, C. Yang, S. Wu, J. Cheng, In-situ fabrication of $g\text{-C}_3\text{N}_4/\text{MIL}-68$ (In)- NH_2 heterojunction composites with enhanced visible-light photocatalytic activity for degradation of ibuprofen, *Chem. Eng. J.* 391 (2020) 123608.
- [180] S. Miao, H. Zhang, S. Cui, J. Yang, Improved photocatalytic degradation of ketoprofen by $\text{Pt}/\text{MIL}-125$ (Ti)/Ag with synergetic effect of Pt-MOF and MOF-Ag double interfaces: mechanism and degradation pathway, *Chemosphere* 257 (2020) 127123.
- [181] R. Bariki, D. Majhi, K. Das, A. Behera, B.G. Mishra, Facile synthesis and photocatalytic efficacy of $\text{UiO}-66/\text{CdIn}_2\text{S}_4$ nanocomposites with flowerlike 3D-microspheres towards aqueous phase decontamination of triclosan and H_2 evolution, *Appl. Catal. B Environ.* 270 (2020) 118882.
- [182] H. Fakhri, H. Bagheri, Two novel sets of $\text{UiO}-66@$ metal oxide/graphene oxide Z-scheme heterojunction: insight into tetracycline and malathion photodegradation, *J. Environ. Sci.* 91 (2020) 222–236.
- [183] S.S. Chen, C. Hu, C.H. Liu, Y.H. Chen, T. Ahamad, S.M. Alshehri, K.C.W. Wu, De Novo synthesis of platinum-nanoparticle-encapsulated $\text{UiO}-66\text{-NH}_2$ for photocatalytic thin film fabrication with enhanced performance of phenol degradation, *J. Hazard Mater.* 397 (2020) 122431.
- [184] S. Zhang, M. Du, Z. Xing, Z. Li, K. Pan, W. Zhou, Defect-rich and electron-rich mesoporous Ti-MOFs based $\text{NH}_2\text{-MIL}-125$ (Ti)@ $\text{ZnIn}_2\text{S}_4/\text{CdS}$ hierarchical tandem heterojunctions with improved charge separation and enhanced solar-driven photocatalytic performance, *Appl. Catal. B Environ.* 262 (2020) 118202.
- [185] Y. Li, Y. Fang, Z. Cao, N. Li, D. Chen, Q. Xu, J. Lu, Construction of $g\text{-C}_3\text{N}_4/\text{PDI}@$ MOF heterojunctions for the highly efficient visible light-driven degradation of pharmaceutical and phenolic micropollutants, *Appl. Catal. B Environ.* 250 (2019) 150–162.
- [186] G. Li, Y. Wang, R. Huang, Y. Hu, J. Guo, S. Zhang, Q. Zhong, In-situ growth $\text{UiO}-66\text{-NH}_2$ on the Bi_2WO_6 to fabrication Z-scheme heterojunction with enhanced visible-light driven photocatalytic degradation performance, *Colloids Surf. A Physicochem. Eng. Asp.* 603 (2020) 125256.
- [187] H. Li, C. Zhao, X. Li, H. Fu, Z. Wang, C.C. Wang, Boosted photocatalytic Cr (VI) reduction over Z-scheme MIL-53 (Fe)/ $\text{Bi}_{12}\text{O}_{17}\text{Cl}_2$ composites under white light, *J. Alloys Compd.* 844 (2020) 156147.
- [188] N. Li, H. Du, M. Tan, L. Yang, B. Xue, S. Zheng, Q. Wang, Construction of Z-scheme $\text{CuBi}_2\text{O}_4/\text{MIL}-88\text{A}$ (Fe) heterojunctions with enhanced LED light driven photocatalytic Cr (VI) reduction and antibacterial performance, *Appl. Surf. Sci.* 614 (2023) 156249.
- [189] D. Roy, S. Neogi, S. De, Mechanistic investigation of photocatalytic degradation of Bisphenol-A using MIL-88A (Fe)/ MoS_2 Z-scheme heterojunction composite assisted peroxymonosulfate activation, *Chem. Eng. J.* 428 (2022) 131028.
- [190] T.A. Quach, J. Becerra, D.T. Nguyen, M. Sakar, M.H. Vu, F. Dion, T.O. Do, Direct Z-scheme mediated $\text{SmVO}_4/\text{UiO}-66\text{-NH}_2$ heterojunction nanocomposite for the degradation of antibiotic tetracycline hydrochloride molecules under sunlight, *Chemosphere* 303 (2022) 134861.
- [191] G. Wu, Q. Liu, L. Ma, L. Tian, J. Ran, Y. Pan, W. Xing, The promoted organic pollutant and visible-light-driven photocatalytic degradation efficiency of MIL-101 (Fe)/ Bi_2WO_6 Z-scheme heterojunction assisting and mechanism, *Colloids Surf. A Physicochem. Eng. Asp.* 656 (2023) 130413.
- [192] L. Cheng, M. Xie, Y. Sun, H. Liu, Bi_2WO_6 -wrapped 2D Ni-MOF sheets with significantly improved photocatalytic activity by a direct Z-scheme electron transfer, *J. Alloys Compd.* 896 (2022) 163055.
- [193] N. Askari, M. Beheshti, D. Mowla, M. Farhadian, Fabrication of $\text{CuWO}_4/\text{Bi}_2\text{S}_3/\text{ZIF67}$ MOF: a novel double Z-scheme ternary heterostructure for boosting visible-light photodegradation of antibiotics, *Chemosphere* 251 (2020) 126453.
- [194] L. Chen, X. Wang, Z. Rao, Z. Tang, Y. Wang, G. Shi, J. Sun, In-situ synthesis of Z-scheme MIL-100 (Fe)/ $\alpha\text{-Fe}_2\text{O}_3$ heterojunction for enhanced adsorption and visible-light photocatalytic oxidation of O-xylene, *Chem. Eng. J.* 416 (2021) 129112.
- [195] X. Dai, S. Feng, C. Ma, L. Xu, L. Fan, Z. Ye, Y. Wang, Direct z-scheme $\text{ZnCo}_2\text{S}_4/\text{MOF}-199$ constructed by bimetallic sulfide modified MOF for photocatalytic hydrogen evolution, *Appl. Surf. Sci.* 639 (2023) 158142.
- [196] S.P. Tripathy, S. Subudhi, A. Ray, P. Behera, G. Swain, M. Chakraborty, K. Parida, $\text{MgIn}_2\text{S}_4/\text{UiO}-66\text{-NH}_2$ MOF-based heterostructure: visible-light-responsive Z-scheme-mediated synergistically enhanced photocatalytic performance toward hydrogen and oxygen evolution, *Langmuir* 39 (2023) 7294–7306.
- [197] H. Xing, J. Shi, W. Yang, Y. Li, R. Wu, J. Wu, Constructing Z-scheme heterojunctions of Zr-MOF/ $g\text{-C}_3\text{N}_4$ for highly efficient photocatalytic H_2 production under visible light, *New J. Chem.* 47 (47) (2023) 21685–21691.
- [198] S. Subudhi, S. Mansingh, G. Swain, A. Behera, D. Rath, K. Parida, HPW-anchored $\text{UiO}-66$ metal-organic framework: a promising photocatalyst effective toward tetracycline hydrochloride degradation and H_2 evolution via Z-scheme charge dynamics, *Inorg. Chem.* 58 (8) (2019) 4921–4934.
- [199] Q. Wei, S. Xiong, W. Li, C. Jin, Y. Chen, L. Hou, D. Tang, Double Z-scheme system of $\alpha\text{-SnWO}_4/\text{UiO}-66$ (NH_2)/ $g\text{-C}_3\text{N}_4$ ternary heterojunction with enhanced photocatalytic performance for ibuprofen degradation and H_2 evolution, *J. Alloys Compd.* 885 (2021) 160984.
- [200] Y. Li, S. Zhu, X. Kong, Y. Liang, Z. Li, S. Wu, Z. Cui, ZIF-67 derived $\text{Co}@\text{NC}/g\text{-C}_3\text{N}_4$ as a photocatalyst for enhanced water splitting H_2 evolution, *Environ. Res.* 197 (2021) 111002.
- [201] P. Zhang, L.J. Wu, W.G. Pan, S.C. Bai, R.T. Guo, Efficient photocatalytic H_2 evolution over NiS-PCN Z-scheme composites via dual charge transfer pathways, *Appl. Catal. B Environ.* 289 (2021) 120040.
- [202] X. Zhang, Z. Chen, Y. Luo, X. Han, Q. Jiang, T. Zhou, J. Hu, Construction of $\text{NH}_2\text{-MIL}-125$ (Ti)/CdS Z-scheme heterojunction for efficient photocatalytic H_2 evolution, *J. Hazard Mater.* 405 (2021) 124128.
- [203] S. Han, Z. Wang, W. Zhu, H. Yang, L. Yang, Y. Wang, Z. Zou, ZIF-Derived oxygen vacancy-rich Co_3O_4 for constructing efficient Z-scheme heterojunction to boost photocatalytic water splitting, *Dalton Trans* 53 (2024) 4737.
- [204] P.A. Koyale, S.P. Kulkarni, J.L. Gunjaker, T.D. Dongale, S.S. Sutar, S.S. Soni, S.D. Delekar, ZnO nanorod/multiwalled carbon nanotube composites sensitized with Cu-based metal-organic frameworks as photoanodes for solar-driven water splitting, *ACS Appl. Nano Mater.* 7 (2024) 2662.
- [205] S. Liang, G. Sui, J. Li, D. Guo, Z. Luo, R. Xu, S. Chen, ZIF-L-derived porous C-doped ZnO/CdS graded nanorods with Z-scheme heterojunctions for enhanced photocatalytic hydrogen evolution, *Int. J. Hydrogen Energy* 47 (21) (2022) 11190–11202.
- [206] Q. Chen, J. Li, L. Cheng, H. Liu, Construction of $\text{CdLa}_2\text{S}_4/\text{MIL}-88\text{A}$ (Fe) heterojunctions for enhanced photocatalytic H_2 -evolution activity via a direct Z-scheme electron transfer, *Chem. Eng. J.* 379 (2020) 122389.
- [207] Q. Ding, D. Xu, J. Ding, W. Fan, X. Zhang, Y. Li, W. Shi, ZIF-8 derived ZnO/TiO_2 heterostructure with rich oxygen vacancies for promoting photoelectrochemical water splitting, *J. Colloid Interface Sci.* 603 (2021) 120–130.

- [208] Y. Dong, X. Wang, H. Sun, H. Zhang, X. Zhao, L. Wang, Construction of a 0D/3D AgI/MOF-808 photocatalyst with a one-photon excitation pathway for enhancing the degradation of tetracycline hydrochloride: mechanism, degradation pathway and DFT calculations, *Chem. Eng. J.* 460 (2023) 141842.
- [209] X. Feng, R. Long, C. Liu, Y. Lu, X. Liu, Flexible Z-scheme heterojunction membrane reactors for visible-light-driven antibiotic degradation and oil-water separation, *Chem. Eng. J.* 471 (2023) 144447.
- [210] J. Low, J. Yu, M. Jaroniec, S. Wageh, A.A. Al-Ghamdi, Heterojunction photocatalysts, *Adv. Mater.* 29 (20) (2017) 1601694.
- [211] Y. Yang, M. Xu, L. Ai, N. Guo, C. Leng, C. Tan, D. Jia, In situ growth of flower sphere Bi₂WO₆/Bi-MOF heterojunction with enhanced photocatalytic degradation of pollutants: DFT calculation and mechanism, *J. Environ. Chem. Eng.* 11 (3) (2023) 109873.
- [212] C. Zhao, Y. Li, H. Chu, X. Pan, L. Ling, P. Wang, Z. Wang, Construction of direct Z-scheme Bi₅O₇I/UiO-66-NH₂ heterojunction photocatalysts for enhanced degradation of ciprofloxacin: mechanism insight, pathway analysis and toxicity evaluation, *J. Hazard Mater.* 419 (2021) 126466.
- [213] Z. Yang, X. Xia, L. Shao, Y. Liu, Efficient photocatalytic degradation of tetracycline under visible light by Z-scheme Ag₃PO₄/mixed-valence MIL-88A (Fe) heterojunctions: mechanism insight, degradation pathways and DFT calculation, *Chem. Eng. J.* 410 (2021) 128454.
- [214] N. Zhang, Q. Zhang, L.Y. Zhang, J.Y. Zhang, Y.Z. Fang, Z. Liu, M. Zhou, Oxygen vacancy induced boosted visible-light driven photocatalytic CO₂ reduction and electrochemical water oxidation over CuCo-ZIF@ Fe₂O₃@ CC architecture, *Small Methods* 6 (7) (2022) 2200308.